COMPUTATIONAL INVESTIGATION OF FREE SURFACE VORTEX FORMATION AT HORIZONTAL POWER INTAKE OF SAMANALA HYDRO POWER STATION

Fernando N. T.

(148354 M)

Master of Science in Engineering

Department of Mechanical Engineering

University of Moratuwa
Sri Lanka

September 2018

COMPUTATIONAL INVESTIGATION OF FREE SURFACE VORTEX FORMATION AT HORIZONTAL POWER INTAKE OF SAMANALA HYDRO POWER STATION

Fernando N. T.

(148354 M)

Thesis submitted for partial fulfillment of the requirements for the Master of Science in Engineering degree

Department of Mechanical Engineering

University of Moratuwa

Sri Lanka

September 2018

DECLARATION

I declare that this is my own work, and this thesis does not include material from any previous submission of a third-party for a diploma or degree of any University or institute. This thesis does not contain previously published material from books, articles or research papers except where proper acknowledgement is made in the text.

Further, I hereby grant the University of Moratuwa, the non-exclusive right to reproduce and distribute my thesis, in whole or part in print, electronic or other medium while retaining the right to use this content for my future endeavors.

Signature: ..... Date: .....

N. T. Fernando

The above candidate has carried out research for the Master's Thesis under my supervision

Signature: ..... Date: .....

Dr. R. A. C. P. Ranasinghe

ABSTRACT

Analysis of free surface vortices formation in a horizontal type water intake structure of Samanala Power Station has in this study been carried out with the help of "Flow-3D" Computational Fluid Dynamic software. A numerical model was validated by using a physical model with horizontal protruded intake which is similar to the construction of Intake of the Samanala Power Station. The numerical model successfully captured the free surface vortex position during the validation process. The surface depression was not captured, however the tangential velocity distribution along the radial distance through the center line of the vortex, which was formed during the physical experiment, was in a good agreement with the tangential velocity distribution of Rankine Compound Vortex, where the middle of the vortex has a rotational flow field (forced vortex) and outside of the vortex it has an irrotational flow field (free vortex). After that, the model has been used to investigate the free surface vortex formation of the Samanala Intake. The intake was modeled by using "Solidworks" software. Due to unavailability of actual terrain data of the pond, I have considered the following: distance from the Dam, the depth of the pond and the intake side abutment angle, as the major parameters to be modeled during the pond modeling. Simulations were carried out to identify the formation of free surface vortices and their properties and characteristics by varying the submergence and fixing the flow rate to the maximum flow of the intake.

ACKNOWLEDGEMENT

This research was carried out under the supervision of Dr. R. A. C. P. Ranasinghe, Department of Mechanical Engineering, University of Moratuwa. I am very much grateful to Dr. R. A. C. P. Ranasinghe for providing me with the guidance, motivation and support throughout the research. I admire his kind-hearted co-operation and encouragement extended at every stage of the study. I wish to thank Dr. Himan Punchihewa for his continuous engagement with the students to successfully complete the research. Furthermore, I would like to express my appreciation to Mr. A. K. Samarasinghe, General Manager (Ceylon Electricity Board), and acknowledge his support and encouragement for this study. Finally, I acknowledge all lecturers and teachers that have imparted valuable support and knowledge to us.

TABLE OF CONTENTS

LIST OF FIGURES

LIST OF TABLES

CHAPTER 1. INTRODUCTION

1.1. Background

Being the first Hydro Power complex, as well as having the first ever public electricity generating units in Sri Lanka, Laxapana Complex plays a major role in feeding the national electricity grid. The complex consists of a cascade of four hydro power stations operating in the Kelani river basin. Figure 1.1. shows the cascade and associate power stations. The complex has two major reservoirs, namely Castlereagh and Maussakele, with higher capacity, mainly for the purpose of reserving water for electricity generation for a longer period of time. On the other hand, the other three smaller tanks are just for the daily demand and supply balance of the cascade and they have a lesser capacity. From the operational point of view, these three ponds very frequently operate with more than 90% variation of their available hydraulic head per day (pond levels are varied throughout the day to cater the fluctuating demand of the system) [1]. Therefore, the condition of these ponds and associated hydraulic infrastructures is vital in supplying uninterrupted power supply.

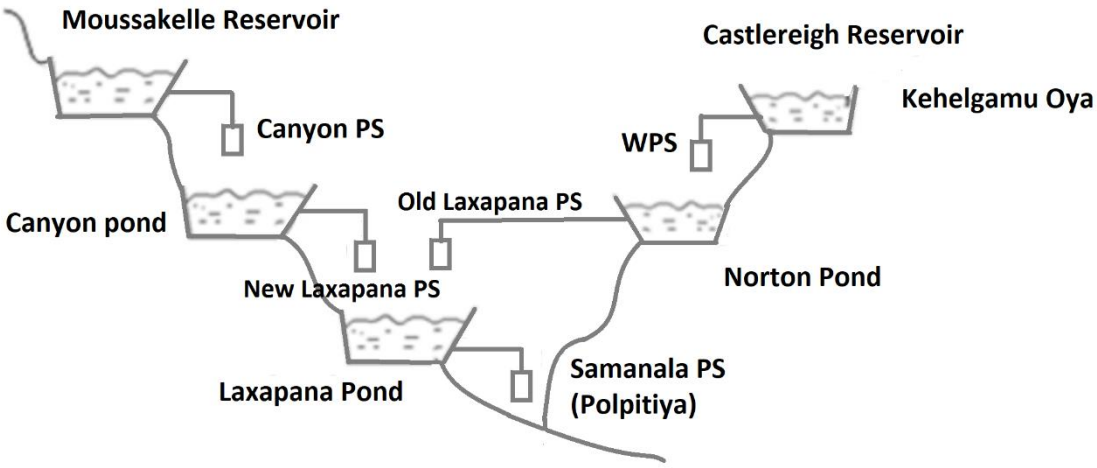

Figure 1- 1: Cascade of Laxapana Complex

Power intake is the initial component to supply water from reservoir to the power plant. Main function of the intake is to withdraw water with a minimum loss of water head to the power tunnel. Furthermore, an additional functional requirement is to

extract clean water to the required extent, without debris and as per the turbine manufacturers recommendations. Basically, there are two types of power intakes, categorized as Horizontal and Vertical.[2]. All the power intakes in Laxapana Complex are horizontal type. Except for the Intakes of Wimlasurendra Power Station in Castlereagh Reservoir and Old Laxapana Power Station in Norton pond, all other intakes are fully submerged and cannot be reached without emptying the reservoir or the pond. Hence, the maintenance works of the intake structures include a chance for immense cost. As per the operational and maintenance records of the Samanala and New Laxapana Intakes at Laxapana and Canyon Ponds, it is evident that blocking of the intake is very frequent during operation. Additionally, formation of free surface vortices is a common phenomenon at Samanala Intake. Cleaning of these intakes requires outages, which restrict plant availability, and frequent blockage of the intakes drops the operational margin (live storage) of the reservoirs.

Preparation of a study to identify and quantify the reasons for these issues and their mitigation activities is essential in order to improve the operational, maintenance and functional requirements of the power stations. Vortex formation is common in Samanala intake. Hence, analysis of vortex formation in free surface, along with its adverse effects and mitigation activities is of utmost importance.

1.1.1. Intake Structure of Samanala Power Station

The intake structure of Samanala hydro power station is located in Laxapana pond. The intake is horizontal type and originally constructed for a maximum flow of 36.5 m^3/s. [3]. A cross section of the intake is shown in Figure 1.2. The intake consists of a steel intake screen (trash rack) which is fabricated with two segments and installed vertically, and around the portal of intake structure is at an angle. Each screen segment is approximately 10 feet (3.0 m) wide and 21 feet (6.4m) in height. The top level of the intake is at 21.4 feet (6.5m) below the Full Supply Level (FSL) of the reservoir. (Elevation 1251.4 ft /381.4 m above Main Sea Level)[4]

Currently, forming of free surface vortex is a frequent physical phenomenon at the intake, even under a relatively higher water elevation. A free surface vortex at

Samanala Intake is shown in Figure 1.3. Operating of Samanala machines under these adverse conditions allows for an entrained air in to the tunnel, which could be harmful for the downstream hydraulic components. Furthermore, there is no Trash Rack Cleaning Mechanism installed for cleaning the Trash Rack. Hence, screens are cleaned manually using portable rakes. In extreme situations, where reaching the intake is difficult, assistance of divers is obtained. However, this will require a total shutdown of Samanala power station and drop down of the pond level from at least 25ft (7.6 m), and up to 30 feet (9.1m) from its full supply Level. Furthermore, operating under higher head losses applies high stresses on the trash racks.

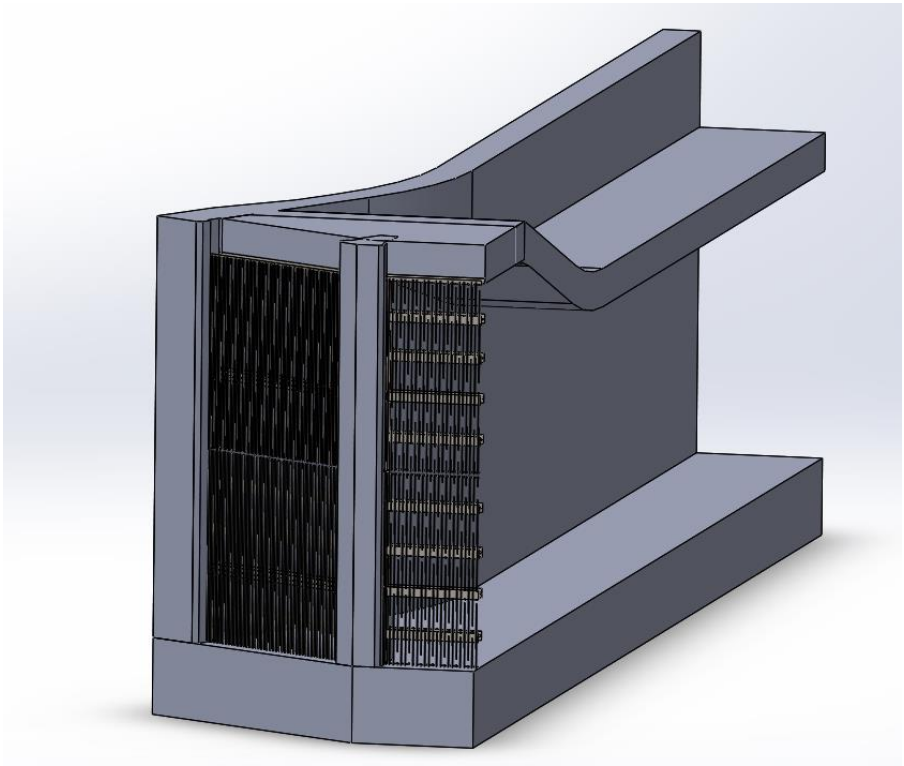

Figure 1- 2: Cross section of Samanala Intake Structure

Figure 1- 3: Free surface vortex at Samanala Hydro Power Intake

1.1.2. Vortex Formation and Drawbacks in Horizontal Type Hydro Power Intakes

Formation of free surface vortices occurs in different kind of hydraulic intakes such as: hydropower intakes, pump sumps and irrigation intakes. These vortices could result in highly negative operational and structural damages on the intake structures, as well as downstream components of its hydraulic system. Many researchers have studied the swirling motion at the intakes to identify its origin, strength, formation, effects and mitigating methods. Knauss [5], Hecker [6] and Durgin and Hecker [7] have identified several causes and published general guidelines. Based on these preliminary studies, several research areas were formed and further studies have been made about the vorticity and vortex formation since then. However, these studies are still an important area of Fluid Engineering, since formation of vortices highly depends on many surrounding factors and is therefore difficult to predict by using numerical or scale down models. [5][6][7][8]

Formation of free surface vortices is prone to have several adverse effects on the intake structures and structures in the hydraulic circuit. The following are some of the related problems in hydropower intakes:

Increasing of Head-loss through the Intake: When vortex is present at the horizontal type hydropower intake, the flow pattern and the distribution of velocity field at the intake are not uniform [9].This non-uniform and swirling flow field is increasing the head-loss through the intake considerably.

Reducing of intake operating range: Since formation of free surface vortices depends on the submergence level, higher submergence level has to be maintained to prevent formation of a vortex. As such full capacity of the reservoir cannot be utilized, it is a major issue for a hydropower station to balance the pond levels conjunction with the required demand.

Air entrainment: Cavitation is one of the major drawbacks for any kind of hydro turbine and its associate components. Formation of free surface vortices may result in air entertainment in the power tunnel and ultimately higher the rate of cavitation of the structure in its hydraulic circuit. Free surface Vortex propagation and its

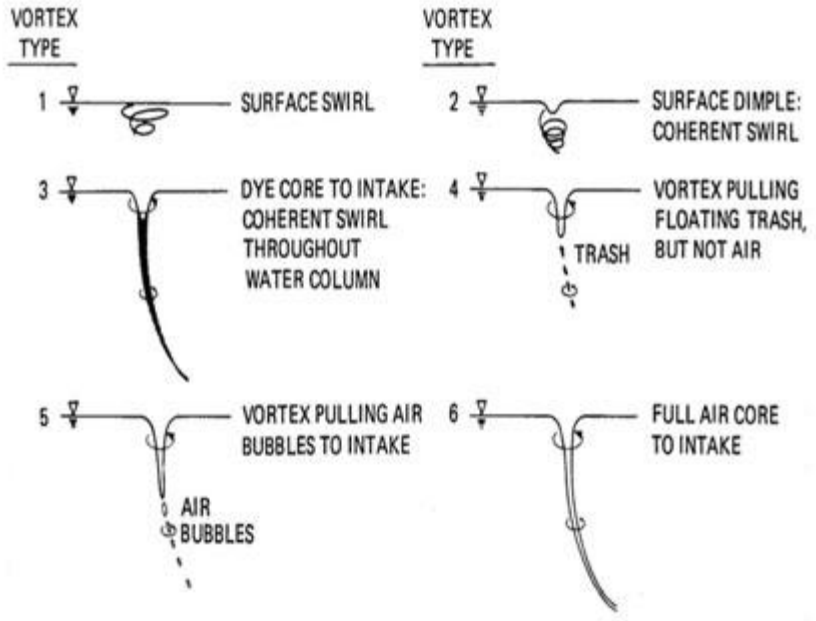

classification according to the strength is given in Figure 1.4. [5]

Figure 1- 4: Classification of Free Surface Vortex Types[5]

Suction of Trash and Debris to the intake trash racks: Clogging the trash racks of the hydraulic intake increases the head-loss through the intake. All types of surface

vortices are able to pull floating matters as well as immersed trash to its direction, depending on its strength of swirling motion, and are able to push them into the intake opening. This trash and debris get trapped on the trash rack depending on the "Clear Spacing" (the gap between two adjacent vertical bars of the trash rack) and increase the "Blockage Ratio" of the screen. This results in possible damages to the trash racks, as well as the intake structure. The figure 1.5 shows the heavily blocked Samanala Intake Trash racks.

Figure 1- 5: Heavily Blocked Samanala Intake Trash Racks

Load fluctuations: Uneven flow distribution and swirling motion due to the presence of vortex fluctuate the desirable flow rate to the hydropower turbine and fluctuate the load.

1.2. Problem Statement

Free surface vortex at the intake is a very frequent and common operational issue in Samanala Power Station. In addition, sedimentation issues and frequent blockage of the trash rack of the intake by river debris also negatively affect the operation of the power station. Higher sediment level of the pond also increases the approaching flow velocity to the power intake, which may be a reason for formation of vortices. These adverse scenarios reduce the operational margins and increase the operational cost of the power station due to frequent outages and operating under partial loads.

Taking an outage for desilting the pond or to carry out modification for the present intake structure will stop the operation of almost all the units of Laxapana Complex, other than Wimalasurendra Power Station. This presents a considerable cost since the power lost from Laxapana complex must be compensated with thermal power. Laxapana unit cost is Rs. 2.44/kWh while the next lowest cost option is Coal Power Plant at a unit cost of Rs. 9.90/kWh[10]. Hence obtaining an outage for such a work is very difficult without presenting proper and reasonable facts and explanations.

During a study, carried out by Japan International Corporation Agency (JICA)[11], in order to identify optimization options of Hydropower Stations in Kelani River Basin, the free surface vortex issue was specifically pinpointed in Laxapana Pond at Samanala Power Intake and it was recommended to study the vortex formation for further remedial actions. Furthermore, after recent rehabilitation of Samanala Power Station, there is a requirement to decrease the clear spacing (Minimum Gap between adjacent Bars of an intake trash rack) of the Laxapana intake trash rack, in order to match the upgraded Francis type Runner[3]. Minimizing the clear spacing leads to increasing the water velocity, and increasing of head-loss, however it is hard to find a study investigating the effects of trash rack spacing for the formation of free surface vortices and vice versa.

Consequently, requirement of a proper study to investigate the Free surface vortex phenomenon at horizontal intake of Samanala Hydro Power Station has been a major requirement in the Laxapana complex. Several management decisions are required,

such as carrying out desilting of the pond, modifying of the intake structure and trash racks, quantifying the energy loss and fixing operational parameters and margins. Hence it is important to study the formation of free surface vortex at the Samanala Intake structure.

1.2.1. Key Objectives

1. Develop a numerical model to investigate the free surface vortex phenomena at Samanala Hydropower Intake
2. Identify and estimate key characteristics and parameters of free surface vortices formed at Samanala Hydropower Intake
3. Estimate safe operating range of the Samanala Power Generating Units in terms of submergence of the intake and the flow rate.

1.2.4. Scope of the Study

The scope of this study is to analyze the formation of free surface vortex at Horizontal type hydro power intake of Samanala Power Station, using Computational Fluid Dynamic (CFD) Software package. Under this scope, validation of numerical (CFD) model and study of the relation between minimum submergence with formation of free surface vortices were carried out at full flow intake conditions.

1.2.5. Outline of the thesis

The first chapter of this study, describes the importance of studying about free surface vortices at hydropower intakes and present situation of the Samanala Hydropower Intake. The theories and literature available for a study of free surface vortices are discussed in Chapter 2. The research methodology followed is discussed in detail under Chapter 3. The results of the study are discussed in Chapter 4 and finally the Conclusion of the study and future activities of the study are discussed in Chapter 5.

CHAPTER 2. REVIEW OF LITERATURE

2.1. Fundamentals of a Free Surface Vortex

2.1.1. Formation of a Free Surface Vortex at Power Intakes

Formation of vortices is due to the spinning motion of the fluid. This spinning motion has to overcome the resistance forces to generate a vortex. Free surface vortices can also form due to the same phenomenon in hydraulic structures. Asymmetric flow is the main reason for the spinning motions. Approaching fluid flow can be blocked, diverted, changed or obstructed due to several reasons to generate an uneven approaching flow field to the intake structures. A wide water channel with smooth walls, where the intake is in the center with uniform approaching velocity, will not create a spinning motion, as all the forces which can create the spinning motions are balanced or very weak. The figures 2.1. and 2.2. show different arrangement of flow fields to create asymmetric flow and produce a swirling motion of the fluid. Item “a” represents asymmetric approaching flow conditions, where the first case is a vertical intake situated asymmetrically in the water channel and the other two are horizontal intakes situated asymmetrically in the water ways, thus creating an asymmetric approaching flow. Item “b” represents a creation of an asymmetric flow condition due to changing of the flow direction before approaching the intake, which is situated symmetrically. However, forming of the vortex depends on the strength of the swirl.

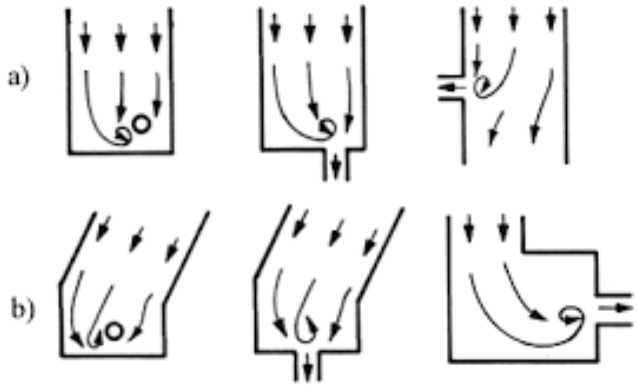

a - Asymmetric Flow Approaching b - Change the direction of flow boundaries

Figure 2- 1: Generating of Swirling Flow 01 [5]

Among the shown method, item “b” of Figure 2-2 represents a special phenomenon of generating swirling motion due to velocity gradient created by Coriolis Forces. [5]

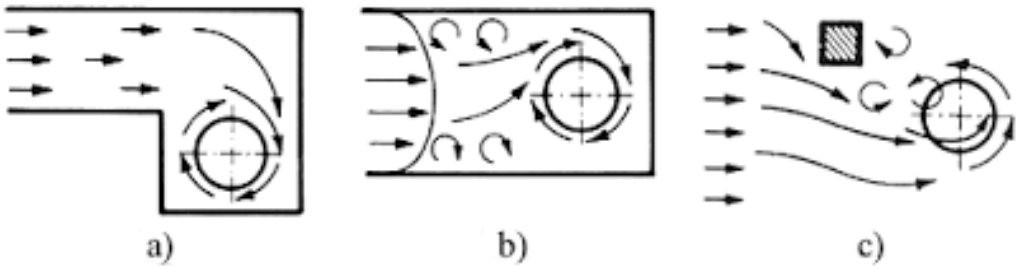

a - Offset Introduction b - Velocity Gradients c - Obstruction

Figure 2- 2: Generating of Swirling Flow 02 [5]

Hydropower intakes are designed to obtain uniform flow to the hydropower tunnel, where the intake geometrical parameters are very critical for creating the required characteristic of the flow field. However, in reality this is not one hundred percent successful. Hence, the intake flows always have some extent of asymmetry. Therefore, hydropower intakes are always prone to formation of vortices.

As per Wu et al.[12], compression and shearing processes are the two main hydraulic actions to generate vortices. In hydraulic intakes fluid flows due to gravity, and according to the amount of opening of wicket gates or needles, which controls the water flow through the hydraulic turbine. This gravitational flow field creates a pressure gradient, such that will draw water in the direction of the intake opening. As a result of this pressure gradient fluid is compressed and fluid particles are forced to rearrange. However, the viscosity of water does not permit rearrangement of fluid particles freely by sliding over each other, and as is present in an ideal fluid. The viscous effect between the two fluid particles creates the required centrifugal force to generate the spinning motion of fluid particles, where the, so-called, shearing action is activated.

As explained above it is evident that primary influencing parameter for the formation of a vortex is pressure, which is correlated to the head over the intake (Submergence). In order to exert the required pressure for the compression and

ultimately for the shearing action, there should be a minimum submergence. However, the amount of submergence also has a maximum limit, where the exerted pressure cannot trigger the spinning motion due to inertia, if the water column is too big.[5]As such, there will be a range of submergence that will allow for the intake vortices to be formed.

Intake geometry, position and the flow rate are the other parameters which influence the hydraulic parameters governing the formation of the vortices. The geometry and the position of the intake directly influence the formation of asymmetry of the approaching flow filed, which is the main factor for originating a vortex, as described earlier. Hence, when designing a power intake these factors should be considered along with the site conditions. Several types of intake arrangements are being used depending on the site requirement. [5]

The specific vortex shape created with the increasing fluid velocity head near the center of the fluid rotation, sacrifices the hydro static pressure. This will cause a drop in the water elevation at the center of the vortex, and the level of drop depends on the strength of the circulation, and this may even form a full air core to the total depth of the water column towards to the intake opening. Anwar [5] has derived an equation to relate the depth of the vortex core from the water surface and the maximum tangential velocity of the vortex core.

$$S = 0.6 \times \left(V_{t,max}\right)^2 / 2g \qquad (1)$$

Where $S$is depth of the Vortex(surface depression)in meters

V_t,$max$is maximum tangential velocity of the vortex core in m/s

In brief, formation of free surface vortices at hydropower intakes depends on the intake geometry, submergence depth, intake position with surrounding structures and the approaching flow field.

2.1.2. Theories associated with Formation of Free Surface Vortices

Hermann Von Helmholtz had studied about the behavior of vortices in inviscid fluids in year 1858[13], [14], [15]. Inviscid fluid is an idealized fluid (Super fluids) with no viscosity where Reynolds number approaches infinity. This assumption can be applied to fluids with very low viscosity and simplify the Navier–Stokes equation to a simpler form called Euler equation. As such, many fluid dynamic flow problems for lower viscosity and higher Reynolds numbers can be solved using the Euler equation easily. Hermann also followed the same process and came up with three theorems which describe the nature of the vorticity of an inviscid fluid or a fluid flow with very low viscosity.

The First vortex theorem of Hermann Von Helmholtz

"*A vortex line is, at any particular time t, a curve which has the same direction as the vorticity vector, at each point of the line."*

$$\Omega = \text{curl}\, V \qquad (2)$$

Where Ω is vorticity vector and V is velocity vector

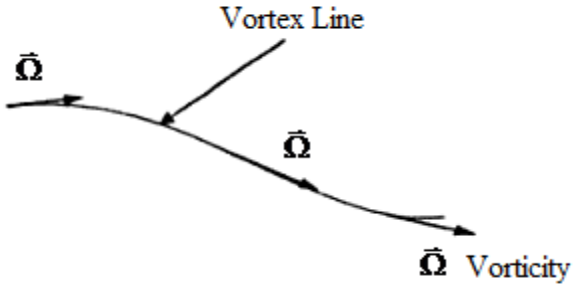

As such the vortex line is tangential to the vorticity vector. Figure 2.3.

Figure 2- 3: Vorticity along vortex line [14]

Mathematically, a vortex line $x = x(s)$, $y = y(s)$ and $z = z(s)$ at a particular time, t is

obtained by solving

$$\frac{\partial x/\partial s}{\Omega_x} = \frac{\partial y/\partial s}{\Omega_y} = \frac{\partial z/\partial s}{\Omega_z} \qquad (3)$$

Thus, the slope of vortex line as projected in x-y plane is equal to

$$\frac{\partial y}{\partial x} = \frac{\Omega_y}{\Omega_x} \qquad (4)$$

Vortex line that passes through every point of a simple closed curve define the boundary of vortex tube (Acheson, 1990) Figure 2.4.

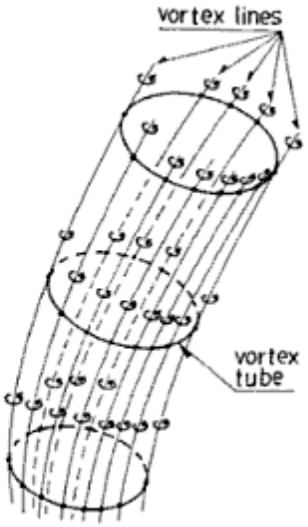

Figure 2- 4: Illustration of vortex tube and vortex line[15]

The Second vortex theorem of Hermann Von Helmholtz

"The fluid elements that lie on a vortex line at some instant continue to lie on a vortex line, i.e. the vortex lines move with the fluid."

Thus, a vortex line cannot end in a fluid, it must therefore extend to the boundaries of the fluid or form a closed loop, or end on a rotating surface *S*at which

$$\Omega=2\omega \qquad (5)$$

Where ω is angular velocity.

The Third vortex theorem of Hermann Von Helmholtz

The third Helmholtz vortex theorem states that

"The quantity

$$\Gamma = \int_S \omega n dS \qquad (6)$$

is the same for all cross-sections S of a vortex tube."

Furthermore, circulation Γisindependent of time.

If the circulation around a closed curve is divided by the areas within the curve, and the area approaches zero as a limit, it may be shown that

$$\lim_{\partial S \to 0} \frac{\partial \Gamma}{\partial S} = \frac{\partial v}{\partial x} = \frac{\partial u}{\partial y} = \Omega \qquad (7)$$

Where, Ω is vorticity component perpendicular to the plane of the elementary area ∂S.

For zero vorticity, there is no rotation of fluid elements, which is the case of free vortex (irrotational flow field). In the highly viscous forced vortex region the vorticity is twice angular velocity (2ω), and the circulation at the matching radius, $r_1$may be calculated based on the flux of vorticity (2ω) across the horizontal plane, πr_1^2, giving

$$\Gamma = 2\pi\omega r_1^2 \qquad (8)$$

Since there is only one constant circulation in the free vortex region, the equation above can be used to calculate the variation of tangential velocity, V_t in the free vortex region as a function of flow conditions in the forced vortex,

$$V_t = \frac{\omega r_1^2}{r} \qquad (9)$$

where r_1 is the core radius and r is the radius of free vortex region respectively

Rankine Combined Vortex

According to Rankine, the simple model of a vortex is given by combination of a rigid body rotation within the core (Forced Vortex), and decay of angular velocity towards outside (Free Vortex). Which means that part of the vortex, i.e. the core of the vortex, is considered as a rigid body (Viscous fluid) which is rotating as a single object and having a circulating flow field around the core (non-viscous fluid)[5],[16].Figure 2.5. describes the regions of a combined vortex.

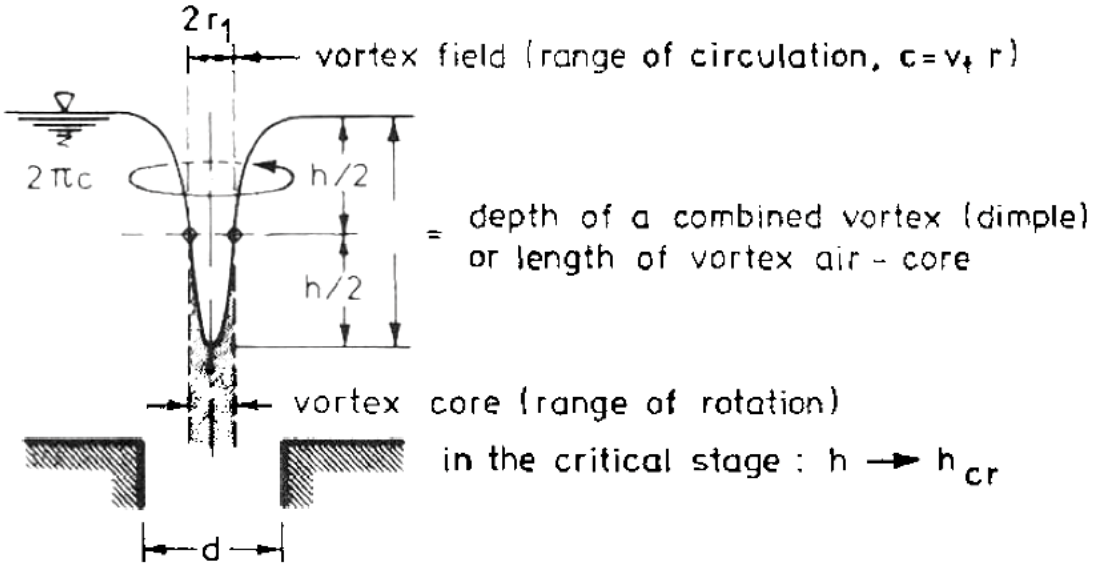

Figure 2- 5: Regions of Combined Vortex[5]

As the definition implies, at the center, where the vortex core is present, the fluid is rotating, so that the tangential velocity, V_t varies linearly with radius

$$V_t = \omega r \qquad (10)$$

Where, ω is an angular velocity rad/s

In the free vortex region, the velocity varies inversely with the radius and directly with

the circulation [5], [16]. According to **Kelvin's theorem:** *"In ideal fluid under a potential body force field, any circuit moving with a fluid conserves its circulation"* [17] Hence, the circulation of a vector flow field, V, along any closed curve, C, is

$$\Gamma = \oint_C^{vdl}. \qquad (11)$$

For circular curve of radius, r,

$$\Gamma = 2\pi r V_t \qquad (12)$$

Therefore;

$$V_t = \frac{\Gamma}{2\pi r} \qquad (13)$$

The variation of tangential velocity and pressure in Rankine combined vortex is given in figure 2.6. [5]

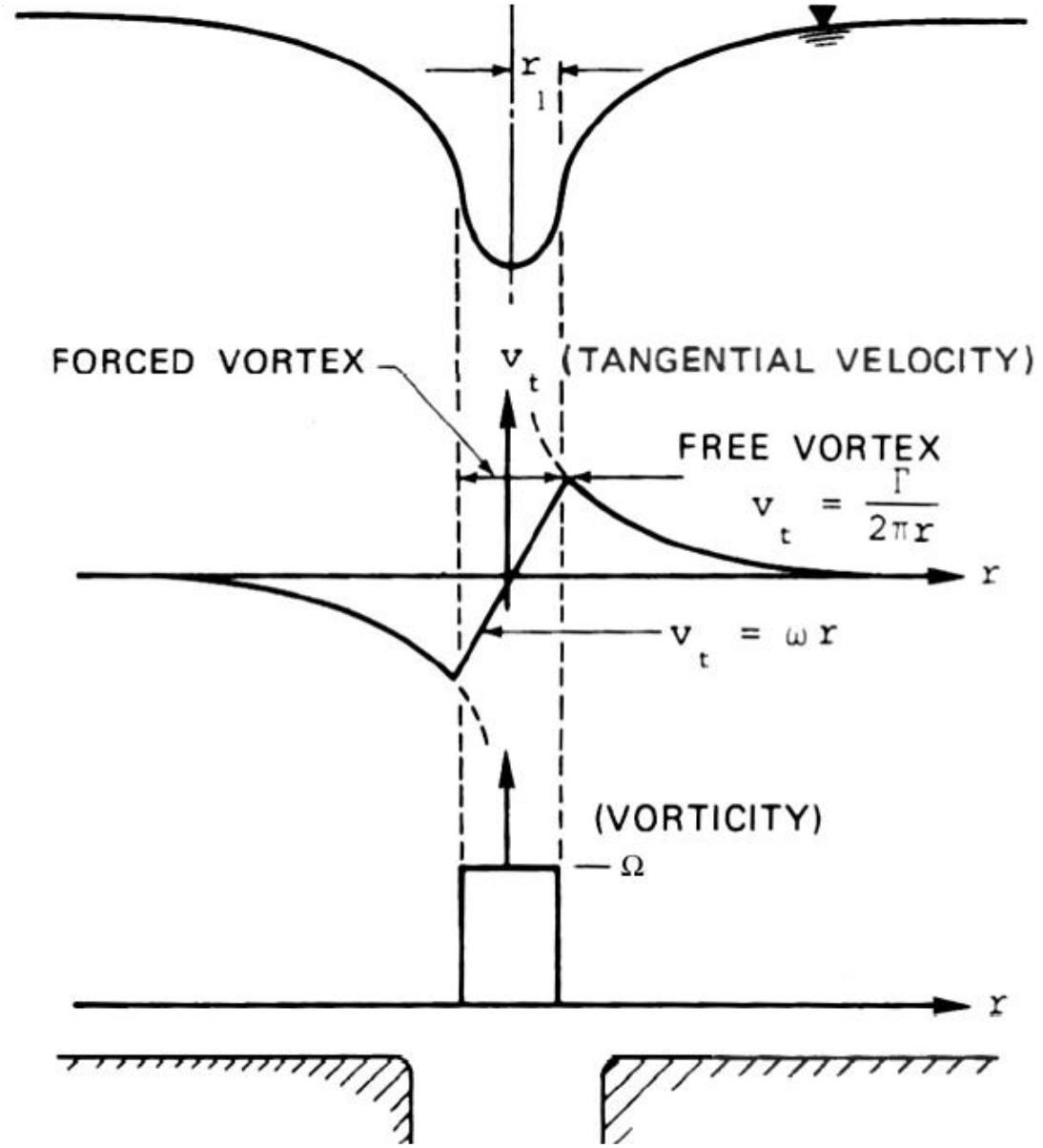

Figure 2- 6: Tangential Velocity Variation of a Combined Vortex [5]

2.1.3. Classification of Free Surface Vortices

Vortices can be classified based on their strength. As per the guidelines developed by Alden Research Laboratory, MA, U.S.A. (ARL)[6]a graphical classification of vortices is presented depending on the strength of the vortex.

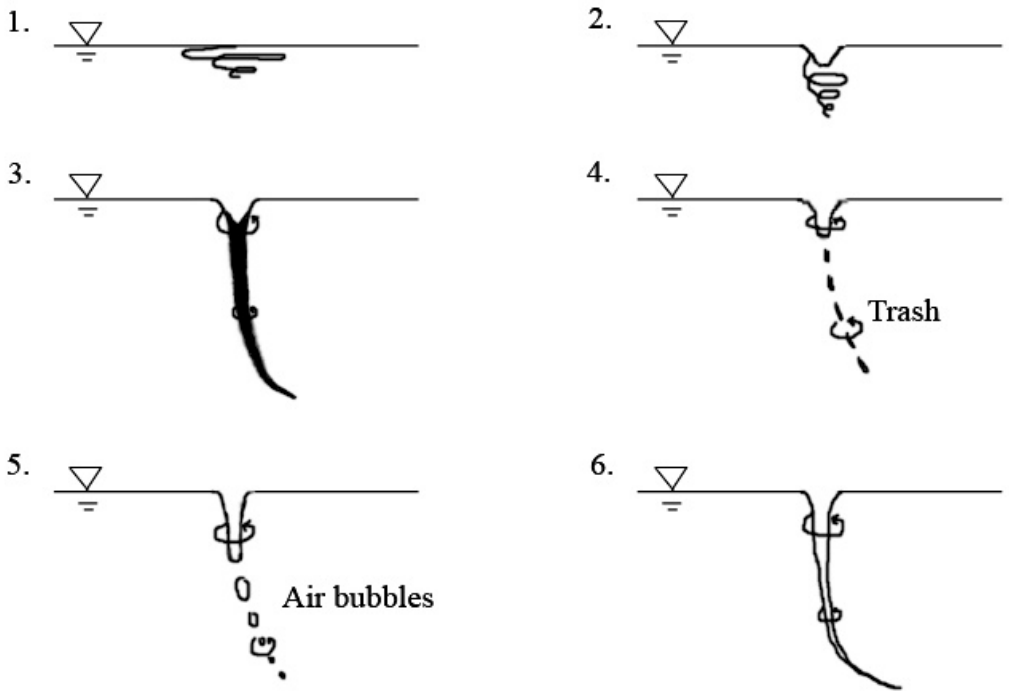

Figure 2- 7: Alden Research Laboratory Classification of Vortices.[6]

Following Table 2.1. describe the classification.

Stage	Name	Description
1	Surface Swirl	A constant swirl on free surface
2	Dimple	A small depression in the center of the swirl
3	Dye Core	Dye core reaches into intake
4	Trash Pulling Core	Vortex pulls floating trash into intake
5	Bubble Entraining Core	Vortex pulls air bubbles into intake
6	Full Air Core	Vortex pulls constant stream of air into intake

Table 2- 1: Description of the Classification given in figure 2.6.[6]

2.1.4. Quantification of Vortex

The strength of the vortex could be estimated by measuring several parameters. These kinds of measurements might be required for optimizing intake designs. The following list represents several parameters that can be measured in a vortex.[18]

- Magnitude of swirl inside the intake pipe.
- Amount of ingested air.
- Changes in entrance loss coefficient or discharge coefficient.
- Free surface velocities around the vortex core.

However, measuring these parameters is not an easy task, as the strength of the vortex and its behavior are rapidly changing in reality. [5]

Most of the time, when measuring small scale intake vortices or even large scale with very low strength, the available methodologies will not give acceptable results or they will not be precise for taking such a small measurement. Furthermore, using a high-end measuring instrument might not be cost effective. [5]Consequently, computational fluid dynamic (CFD) methods are used to study the vortices at a lower cost.

2.2. Hydraulic Scale Models

2.2.1. Introduction to Scale Models

Designing of hydraulic structures is always a challenging task, with a lot of fine-tuning followed by several experiments and testing of physical and mathematical models. Correct and precise testing of the design approaches is essential to acquire the required output with the expected efficiency. At the present moment, two distinguished methodologies are used for this purpose.

i. Conventional Hydraulic Scale Models

ii. Computational Models based on Mathematical models.

Between these two, and in order to test the scale down models of hydraulic structures, Conventional Hydraulic Scaled Models have been more popular for a longer period of time. The improvement of computational power and advancement of the capability to prepare simulated large models, boosted up the popularity of Computational Models to model and investigate complex hydraulic structures. Compared to conventional scale down models, Computational Models require less money and time. Hence, they are more popular and more widely used at the present. However, the main difficulty when using computational models is the difficulty of their accurate application for a completely new model. For an example, in the field of hydropower, every project has its own unique design and requirements, whereas using a model developed for some other project may not be suitable or may not give an accurate result. As such, validation of the models has to be done before applying them to the real situation. Validation may require scale down models, which are sometimes the exact scale down models of the actual structures or similar models. Hence, the present-day studies use hybrid type of approach with both scale down models as well as computational models. [19], [20] As such, study about the scale down models is also an important matter in planning computational models.

As the name implies, scale down models include building a model exactly as the actual one or the prototype with a reduced scale, by achieving relevant properties and similitude to the physical aspects. Most important similitudes are Geometric, Kinematics and Dynamics. Geometric similitudes can be easily obtained by scaling down all the dimensions. Denoting, r_0 for ratio, p for prototype, m for model, V for velocity, a for acceleration and T for time, following ratios (equation 14,15 and 16) can be used for establish geometrical and kinematic similitudes. Kinematic similitudes imply that velocity, acceleration and time are in a constant ratio.

$$L_{r_0} = \frac{L_m}{L_p} \tag{14}$$

$$V_{r_0} = \frac{L_{r_0}}{T_{r_0}} \tag{15}$$

$$a_{r_0} = \frac{L_{r_0}}{T_{r_0}^2} \tag{16}$$

$$T_{r_0} = \frac{T_m}{T_p} \quad (17)$$

Despite the above, dynamic similitudes are associated with the force polygons which are on geometrically equivalent points in both model and the actual situation of the prototype. Acceptable method to obtain dynamic similitudes is using the non-dimensional parameters. [19]For the interest of free surface flow, the most important non-dimensional parameters are, Reynolds Number (Re), Weber Number (We), Froude Number (Fr) and Circulation Number (N_Γ). (Equations 18, 19, 20 and 21), where Re relates to inertial forces with viscous forces, Weber number relates to fluid inertial forces to its surface tension, Fr relates to inertial and gravitational forces and N_Γ, as the circulation number comes in to the screen with swirling free surface flow and denotes the non-dimensional form of the circulation term.

$$Fr = \frac{V}{\sqrt{gD}} \quad (18)$$

$$Re = \frac{QD}{Av} \quad (19).$$

$$We = \frac{\rho Q^2 h}{A^2 \sigma} \quad (20)$$

$$N_\Gamma = \frac{\Gamma D}{Q} \quad (21)$$

Where:

Q is flow rate [m3/s],
A is area of the intake [m2],
V is flow velocity [m/s],
ν is kinematic viscosity [m2/s],
g is gravitational acceleration [m/s2],
ρ is density of the fluid [kg/m3],
σ is surface tension of the fluid [N/m],
D is diameter of the intake [m] and
Γ is circulation [m2/s].

These non-dimension parameters can be used to perfectly match the scaled model and the actual or the prototype. For a perfect model all the non-dimensional

parameters should match with the prototype parameters, which is not possible in actual scenarios due to viscous forces and surface tension. [6]

2.2.2. Computational Fluid Dynamics (CFD)

Researchers have been carrying out several studies to understand the mechanism of intake vortices for a long time by scale model experiments and deriving empirical equations. With recent popularity of computational modeling, more research areas have opened to study and validate the empirical formulas derived from using previous studies. Computational Modeling, mostly referred to Computational Fluid Dynamics (CFD), is based on multidisciplinary package for solving fluid dynamic problems. Three main disciplines, Fluid Mechanics, Numerical Analysis and Computer Science, are integrated into a single package.CFD solves a continuous fluid dynamic problem in a discreet manner. In continuous domain, each flow variable is defined at every point of the domain, in contrast, each flow variables define only at the grid points in discreet domain, where grid is the method to convert the continuous domain to a discreet domain. There are three main approaches to CFD. They are as follows: Finite Difference Method (FDM), Finite Element Method (FEM) and Finite Volume Method (FVM). FDM methodology is used to predict the condition of a particular position after a defined time step in future, using the data available on adjacent nodes at present time with employing a time-distance grid of nodes and truncated Taylor series approach. In contrast, FEM, although initially developed for structural analysis, is utilized to predict the fluid flow, with its capability to use a non-regular grid, hence, it is capable of simulating complex boundary geometries. However, the methodology used for the flow prediction is more complex than in FDM. Ultimately, Finite Volume Method (FVM) has the best attributes of the so-called FDM and FEM. As such it is capable of handling complex boundary geometries and accurately modeling conservation for each cell in the grid. [16]The fundamentals behind the CFD are Navier-Stokes equations, which are the partial differential equations derived from conservation of mass, momentum and energy with appropriate initial conditions and boundary conditions. (Equations 22, 23, 24) These three equations and defined conditions are expressed mathematically using integral or partial differential equations to be solved by a numerical method.

$$\frac{\partial \rho}{\partial t} + \nabla \cdot (\rho V) = S_m \qquad (22)$$

$$\frac{\partial (\rho V)}{\partial t} + \nabla \cdot (\rho VV) = -\nabla p + \nabla \cdot \tau + \rho g + F \qquad (23)$$

$$\frac{\partial (\rho e_t)}{\partial t} + \nabla \cdot (\rho e_t u) = \nabla \cdot q - \nabla \cdot (pu) + \tau \cdot \nabla u \qquad (24)$$

Where:

V is flow velocity,

t is time,

p is static pressure,

τ is stress tensor,

g is gravitational acceleration,

ρ is density of the fluid,

S_m is the source of mass added

F is external body force

Structure of the CFD code has three main components, Pre-Processor, Solver and Post Processor. Solver is the heart of the code where the numerical equations are solved. Pre and Post processors are to create the interface for the user to communicate with the solver and to define the problem and analyze the results. Apart from these major sections, CFD software packages comes with 3D modeling facility, material libraries and various turbulence models which are pre-defined models to represent several turbulence flow conditions.

Solver in all the CFD code is based on FDM, FEM or FVM to solve governing equations using various algorithms and numerical techniques. However, most of the commercially available CFD packages such as FLUENT, FEM, START-CD and FLOW-3D are using FVM method, as the method is well established and validated.FVM integrates the governing equations in the finite volume over the computational domain and therefore one generic equation is available for one flow

variable such as velocity, enthalpy or species concentration [16]For dependent variable ϕ, Exchange Coefficient (Lamina + Turbulent) Γ_ϕ, Flow Velocity Vector $V\phi$, Flow Density ρ and source of the variable $S_\phi$the generic equation can be written as below:

$$\frac{\partial \rho \phi}{\partial t} = -\nabla(\rho V \phi) + \nabla\left(\Gamma_\phi \nabla \phi\right) + S_\phi \qquad (25)$$

To verify the CFD predictions, validation of the developed model against a known flow system is vital. Mathematical/numerical verification with grid dependency validation for the convergence and stability of the model and physical validation of the model with experimental results are the methods to be used for validation of a model. Most of the real-world applications of CFD, therefore, more or less, focus on qualitative comparison with existing flow cases. Hence, experience of the CFD operator is a vital factor to achieve good results. [16]

2.2.3. Factors to be considered during CFD modeling

Explicit Vs Implicit:

These two systems are used to convert governing partial differential equations into an algebraic format in finite difference type approximations. Relatively larger time steps are allowed for the calculations in the implicit method, hence the time requirement for the process can be reduced. However, the implicit method sometimes introduces substantial errors and higher convergence time. Furthermore, the method is not suitable for convective processes. In contrast, the Explicit method requires lesser computational power, although it has time step restrictions. That said, the stability of the system in the explicit method, is governed by the Courant Criterion, which links fluid velocity inside the mesh, time-step size and the internodal distance. In other words, information of a particular cell should be transferred only to the

neighboring cell during a time step. This condition limits the usage of smaller grid size with larger time-steps. Some CFD packages like Flow-3D, control the time steps automatically on their own, while Fluent and CFX provide control to the user to determine the time-step size in addition to the automatic control. Courant number can be defined as follows.[21], [22]

$$C = a\left(\frac{\Delta t}{\Delta x}\right) \qquad (26)$$

Where: C = Courant number

a = Velocity Magnitude

Δt = Time step size

Δx = Length between mesh elements

For the above explained criteria $C \leq 1$.

Fluid Solid interface:

Since the flow near the fluid/solid interface is more complex due to the presence of turbulence and the wall shear stresses at the surface and within the boundary layer, the size of the mesh size can significantly affect the accuracy of the calculations. Further separate meshing might be required to the interface, in order to obtain the required accuracy.

Selecting the appropriate physical model and the Boundary Conditions:

CFD developers include several physical models and boundary conditions to the package to make the system user friendly. It is important to select the appropriate physical models as well as boundary conditions to obtain the correct results. As an example, there are several models developed to model the turbulence of the fluid flow. However, application of the model is highly depending on the particular case.

2.3. CFD modeling of Intake Vortices

CFD has been used to study intake vortices for the past two decades, owing to a rapid advancement of the computational power. Rajendran et al.[23] carried out a study to compare the physical and numerical models of a pump sump. While the numerical model is based on Reynolds averaged Naiver-Stokes equations, the physical model is equipped with a turbulent flow regime. Flow visualization of the experimental model is carried out by using a particle image velocimetry and dye. A single free surface vortex was observed with a difference in the size of the vortex compared to the physical and numerical models, during the study. Figure 2-8

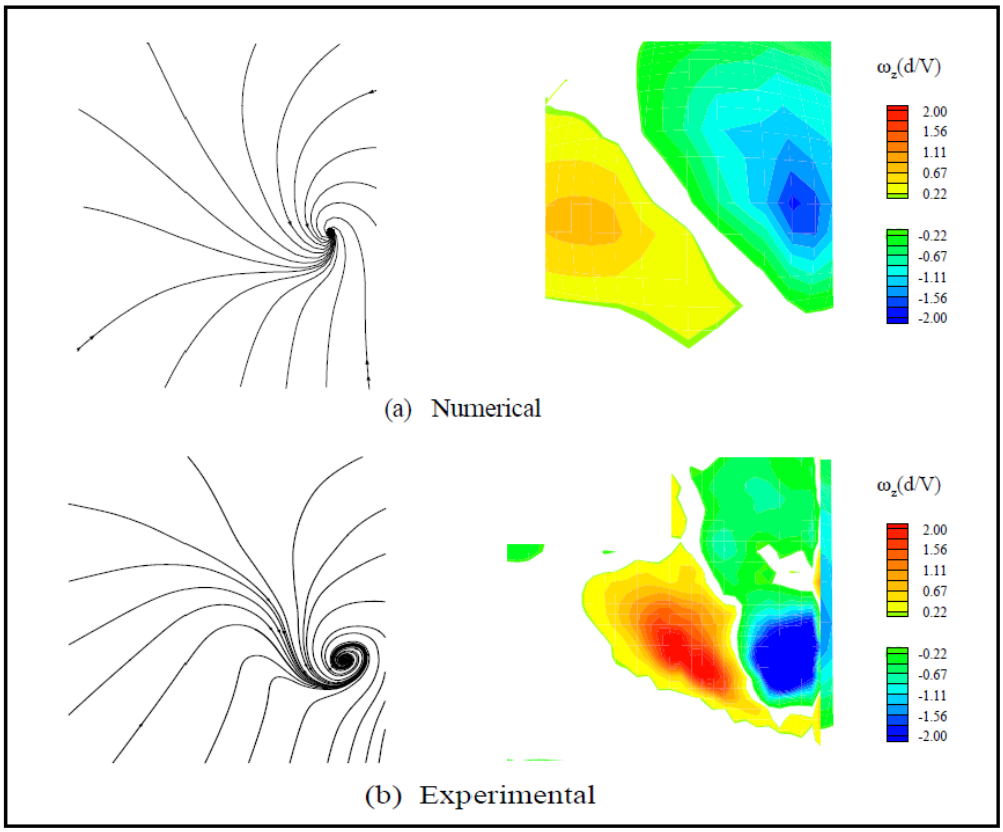

Figure 2- 8:Comparison of Experimental and Numerical Results [23]

Suerich et al.[24] studied about free surface vortices at hydropower intake using experimental and numerical analysis. Experimental setup was built as a simplified

intake with a 3-inch intake pipe and Ansys-CFX 10.0 software package used for the numerical simulation. Two experimental setups were tested: 1st one with protruded intake pipe, low water level and higher flow rate to match the higher intake Froude number and then the second case is with flushed intake entrance with the wall and two side piers from left and right to the intake, with relatively low intake Froude number. During the numerical simulation, water depth was maintained adjusting the imposed pressure at the outlet, while inlet boundary condition was maintained as velocity inlet and the set water level. Strong vortices were observed even with the lower Froude number in the second case. Furthermore, it was observed that the vortex was unsteady throughout the simulation under transient mode. Figure 2-9.

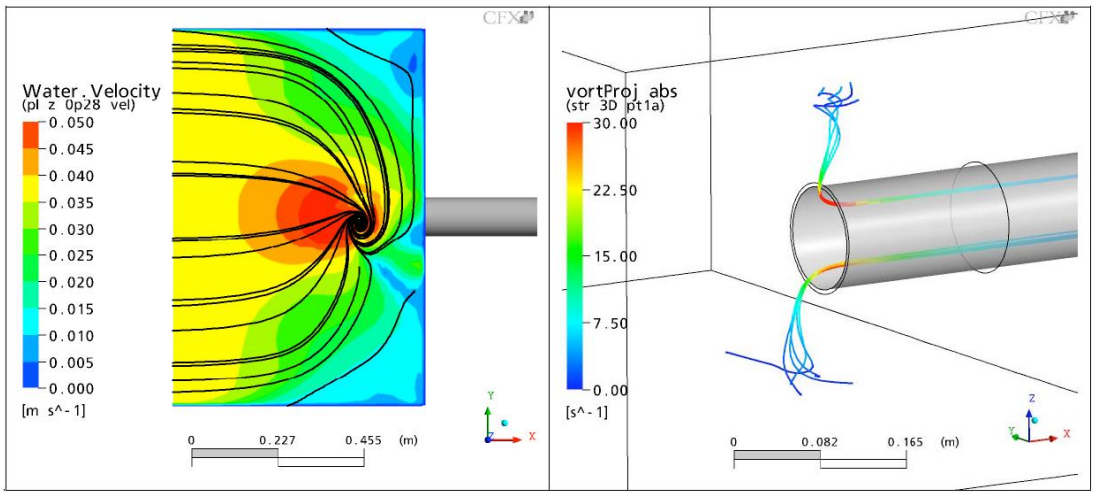

Figure 2- 9: Surface 2D stream lines and 3D stream lines of the unsteady vortices [24]

Skerlavaj et al. [25]compared Turbulence models for surface vortex simulation in pump sumps using Ansys CFX 12.1. The following different turbulence models were tested:

- Eular Model
- Laminar Model
- SST (Shear Stress Transport) Model
- SST-CC (Shear Stress Transport with Curvature Correction) Model

- SAS-CC (Scale Adaptive Simulation with Curvature Corrections) Model
- LES Model

In conclusion, they declared that SAS-CC model would be the most suitable turbulence model to investigate surface vortices of pump sumps. However, the results of the other models also closely agreed with SAS-CC, except for SST-CC.

Hribernik et al.[9], studied about the optimization options for Trash racks of Hydropower Plant intakes. Ansys-CFX 12 solver was used for the numerical simulation to investigate the velocity profile ahead of the trash racks. A vortex was observed ahead of the intake and it resulted in uneven velocity distribution on trash racks despite of symmetric ideal velocity distribution. Figure 2-10

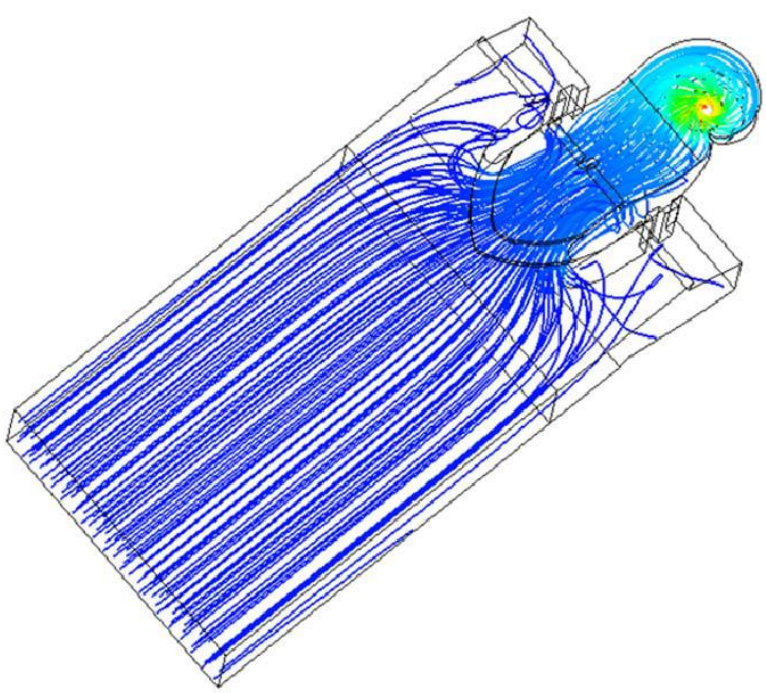

Figure 2- 10: Stream lines of flow distribution along the intake trash racks [9]

Lucinoet al. [26]successfully used Flow-3D CFD software to detect vortices in pumps sump. Very stable submerged vortices were identified and it was explained that they were due to the geometric condition and not depending on the level of submergence when compared to the free surface vortices. Large Eddy Simulation (LES) was the turbulence model used and Split Lagrange was the free surface tracking model. The fluid was considered monophasic and incompressible.

Bayeul-Laine et al. [27] studied the flow stream in water sump pumps using a Star CCM+ V6.06CFD software package. A two phases model was used with air and water VOF method, in order to track the free surface while using both SST k-ω and Realizable Two-Layer k-ε models as turbulence models. It mainly tested the ability of detecting free surface vortices and air entertainment to the pump using the above software. According to the study it is concluded that catching up the occurrence of vortices is really difficult, due to highly unsteady, unstable and intermittent results regardless of the selected turbulence model.

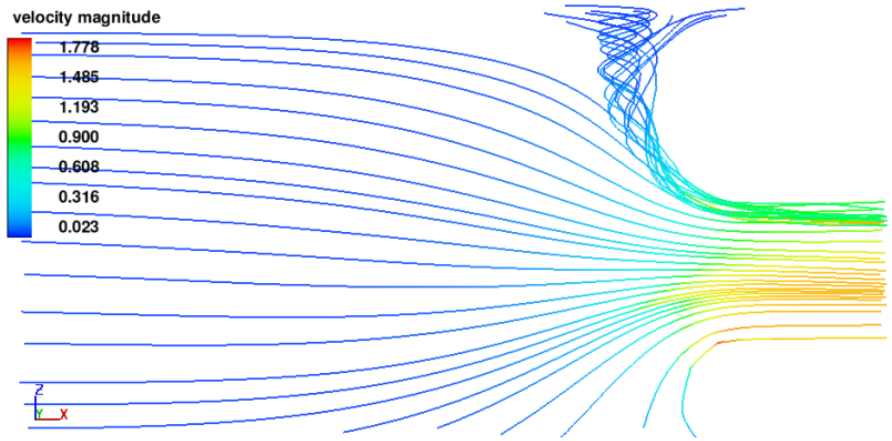

Figure 2- 11: Computed Streamlines for Intake Froude Number 1.2[28]

Hamed et al. [28] analyzed the flow in a reservoir in the presence of a vortex. Flow 3D CFD package was used with VOF and LES models. Hexahedral mesh was used as computational domain and Fraction Area/Volume Obstacle Representation (FAVOR) method was used to define the reservoir walls and the intake. Model was tested for two intake Froude numbers, respectively 0.6 and 1.2. Vortices generated

by using the CFD closely matched with the Rankine vortex model theory (Rankine 1858). The CFD model caught the spiral motion of the free surface vortex without the dimple effect (water surface depression) at the center of the vortex. However, the experimental results and the numerical results were in good agreement.

2.4. Engineering measures related to free surface Vortices at Intakes

The prevention of the intake vortices is discussed in [29] and [30]. The main targeted measures are providing enough intake submergence to minimize the surface velocities and in order to minimize the swirling tendency of the flow, alongside with the setup of the approaching flow conditions symmetric, as much as possible by correctly placing the intake in the reservoir or the channel with including proper guidance of the flow and using anti-vortex devices such as submerge raft, floating raft, Extended plate type, wedge type and covered intake type vortex suppressors. As such, it is evident that preventing free surface vortices at intakes can be controlled by correct design of the intake structure, correct placing of the intake structure and by providing the suitable vortex suppression devices.

2.4.1. Submergence of the Intake

As discussed, submergence level of the intake from the free surface level is an important factor to be considered in designing hydropower intakes. Several studies have been carried out to find the relationship and the effect of the submergence to the formation of free surface vortices. Jain et al. [31] defined the term critical submergence as the minimum submergence level of the intake to prevent it from forming air entertaining free surface vortices. Carlos [32] developed a formula to find out the critical submergence as a function of Reynolds number and the Weber number. Liu et al [33] studied about the vertical intakes with different intake geometries to find out their effects on submergence requirements, and have carried out dimensional analysis to find out the parameters influencing the free surface

vortices, based on past literature and by taking critical submergence as the dependent parameter of the analysis.

$$S = f(D, D_o, Q, \Gamma, \rho, \mu, \sigma, g, \delta_i) \quad (27)$$

Where; D = Diameter of the pipe intake

D_o= Diameter of the bell-mouth intake

Q = Discharge of the intake

Γ = Circulation

ρ = Density of the Fluid

μ = Dynamic viscosity

σ= Surface tension of the fluid

g = Gravitational Acceleration

δ_i= Length Parameter, distance from side walls, length of approach side walls, height of the bell-mouth, etc.

Schematic representation of the above variable is shown in figure 2-12.

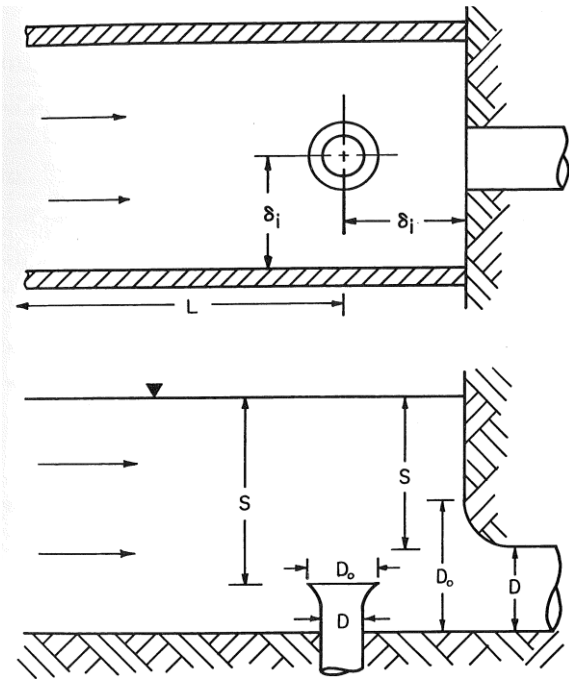

Figure 2- 12: Schematic representation of horizontal and vertical intake configurations

Furthermore, several empirical formulas exist for evaluating the critical submergence of the water intakes. Hecker [6], Knauss [5]Gordon [29] have developed a formula to define the critical submergence level as a function of an average velocity and the diameter of the intake as defined in Figure 2-13.

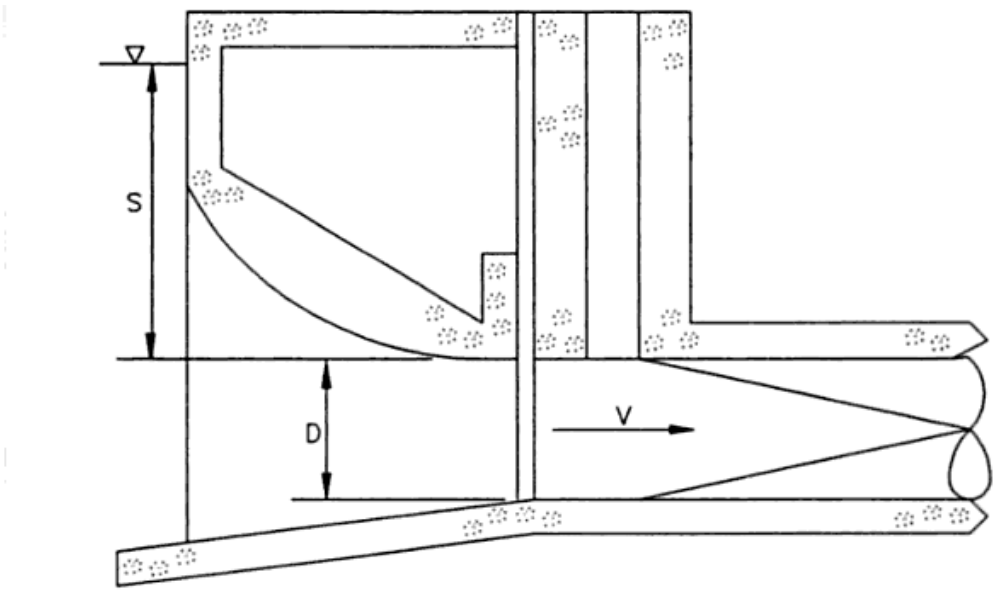

Figure 2- 13:Horizontal intake with "S" level of submergence.

$$S = kVD^{1/2} \qquad (28)$$

Where: S = submergence level required to prevent air entertaining vortices (ft)

D = Height of the intake gate (ft)

V = Average Velocity at intake gate (ft/sec)

k = 0.3 for symmetrical approached flow and 0.4 for unsymmetrical approached flow.

Reddy and Pickford [29]derived a relationship between critical submergence and the Froude number (Fr) at pump sumps and have indicated that the ratio of S/D ranges from Fr, when using vortex prevention devices and 1+ Fr otherwise. Pennino and

Hecker [29] found that it is difficult to derive a specific criteria for the minimum submergence, due to various approaching geometries and topography at the pump storage intakes and proposed to maintain the value as in equation (28).

$$\frac{V_o}{\sqrt{g\mathrm{S}}} < 0.23 \qquad (29)$$

Where: V_o = The bell-mouth intake velocity

S = The submergence to the centerline

However, Gulliver, Rindels and Lindblom [29]suggested that the application of the above formulas is very limited because of different approaching conditions. They have identified a relatively safe region to prevent from free surface vortices at horizontal intakes. It was defined by the following equations (30,31)

$$\mathrm{S} > 0.7D \qquad (30)$$

$$\frac{V_o}{\sqrt{g\mathrm{S}}} < 0.5 \qquad (31)$$

Where: S = Submergance measured from the water surface to the point of intersection of the soffit bellmouthwitha linedrawn perpendicularto the water surface between the bellmouth bottom and the bellmouth soffit.

D = The minimum diameter to which the bellmouth narrows

V = Velocity measured in the intake at the location where submergence is measured

These parameters are defined in the following Figure 2-14.

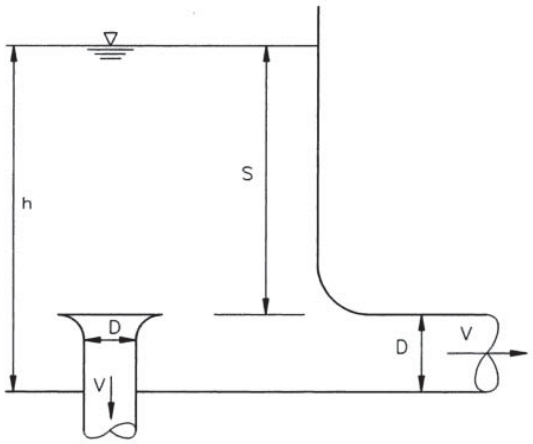

Figure 2- 14:Horizontal and vertical intake submergence

Knauss [5] has developed an analytical formula for four types of intakes arrangements of vertical, vertical inverted, horizontal and inclined intakes, which is defined in figure 2-15.

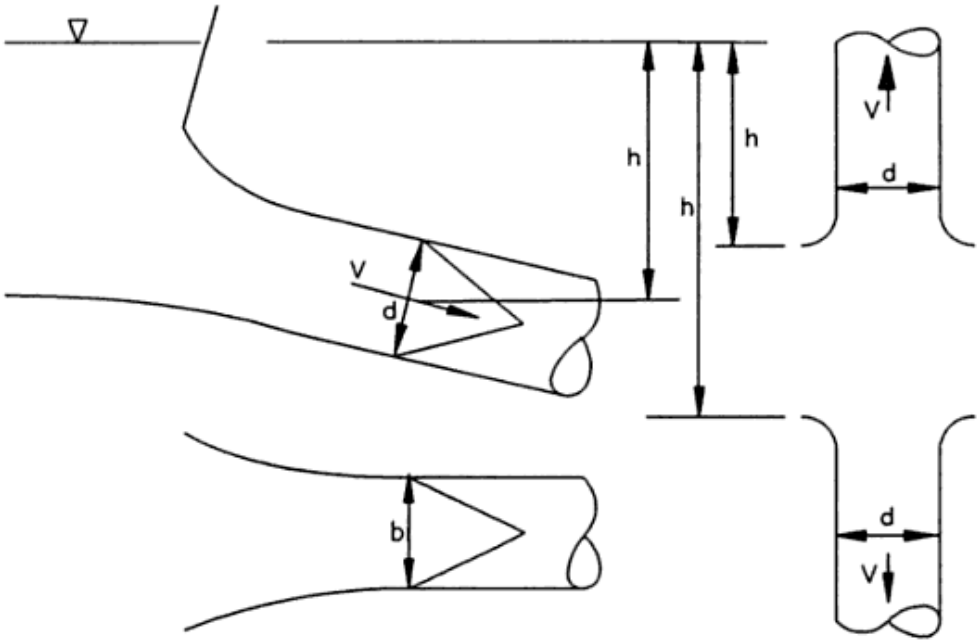

Figure 2- 15: Illustration for Knauss's critical submergence formula

Following is the analytical formula which he defined

$$\left(\frac{\mathrm{h}}{D}\right)_{critical} = \frac{kc}{D^{3/2}\sqrt{g}} = kN_cFr \qquad (32)$$

Where: k = Constant representing the gradient of the liner relationship

h = Depth of water above the centerline of intake at the face of the intake

D = Diameter or the characteristic dimension of the intake

Fr = Froud number

$N_c = V_t r/V_d$

V_d= Intake velocity

V_t = Tangential velocity of approach flow

r = radius of the vortex

Knauss also emphasized the requirement of suitable approach flow condition to minimize circulation and came up with two relationships for minimum submergence requirements for the intakes, with normal approaching flow to confirm non-formation of intake vortices without anti-vortex devices. As per the findings the following formulas were obtained.

$$\left(\frac{\mathrm{h}}{D}\right)_{critical} = 1\ to\ 1.5, Fr \leq \frac{1}{3} \qquad (33)$$

$$\left(\frac{\mathrm{h}}{D}\right)_{critical} = 0.5 + 2Fr, Fr > \frac{1}{3} \qquad (34)$$

Using the above two relations, Knauss developed that two intake models depend on the capacity of the intake. For a larger intake with low main velocity, 2m/s, such as hydropower intakes, equation 33 is proposed. While, equation 34 is applicable for smaller intakes with relatively higher mean velocities, 4m/s, such as pump intakes and cooling water intakes. As such, the following graph in figure 2-16. was developed based on the above two equations. Using the above two relations Knauss developed that two intake models depend on the capacity of the intake. For larger

intakes with low main velocity, 2m/s, such as hydropower intakes, equation 33 is proposed. While equation 34 is applicable for smaller intakes with relatively higher mean velocities, 4m/s, such as pump intakes and cooling water intakes. As such the following graph in figure 2-16. was developed based on the above two equations.

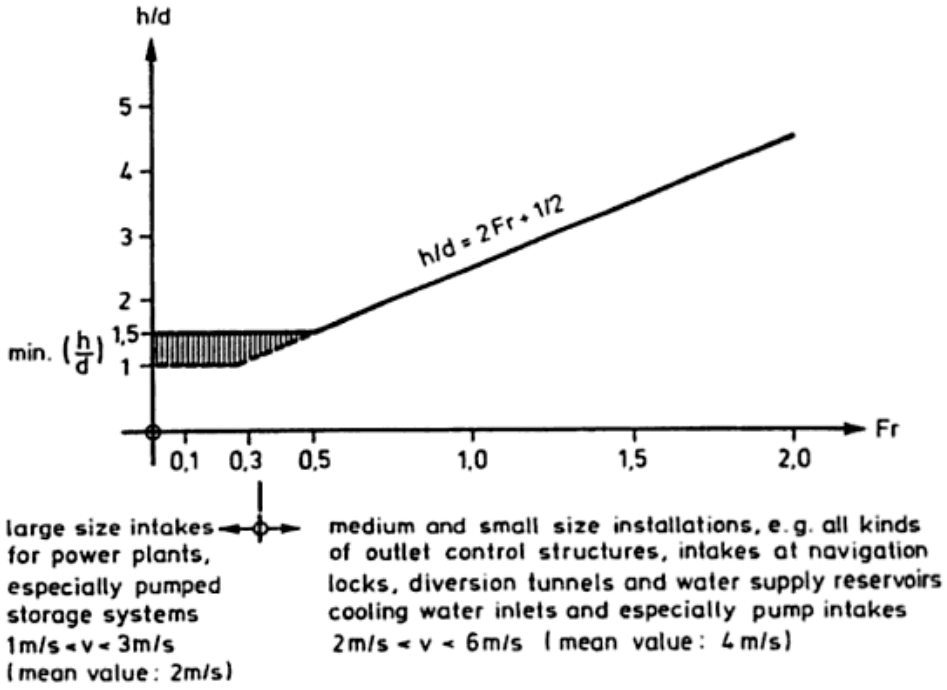

Figure 2- 16: Recommended submergence for the intakes[5]

Later, Hecker's formula for the critical submergence was devolved, based on the Knauss formula and the researches carried out by Gordon and Knauss [29] ,. Equation (35).

$$\left(\frac{h}{D}\right)_{critical} = 1 + 2.3Fr \qquad (35)$$

Finally, as per the ASCE [29], for horizontal intakes the criteria developed is $S/D > 2$ for all the arrangements.

2.4.2. Surface Tension

Many studies have been carried out to identify the effect of the surface tension of the fluid to formation of free surface vortices. Most of the studies concluded that surface tension effect is negligible. Alan J. Rindels and John S. Gulliver[30], Dagget and Keulegan [29] revealed that in the range of Reynold Number from $3x10^3 7x10^5$ surface tension does not affect the formation of vortices. Yildrin and Jain[29] found that surface tension is only an important parameter near to the core of the vortex with lower circulation using analytical method. Jain et al.[29]also concluded that for a cylindrical tank surface tension is not an important parameter in the range of $120 < \rho(\frac{V^2 D}{\sigma}) <$ 34,000. Anwar [29]came up with a study to identify the effect of the surface tension relating to the Weber number and found that, the surface tension effects are negligible, if the Weber number is greater than $1.5x10^4$. It is an important parameter only when a surface depression is available. Therefore, it can be concluded that surface tension does not highly affect the formation of vortices at intake structures except for the above described special cases.

CHAPTER 3. RESEARCH METHODOLOGY

Selection of the CFD code (software package) was a challenging decision, since the suitability of the software for modeling the specific application, affects the usability, performance, reliability and accuracy of the simulation. Literature reveals that, many codes have been used for past studies and have succeeded with a different model arrangement. Suerich et al. [24]used Ansys CFX 10.0 with k-ε turbulence model with wall functions, Hribernik et al. [9]used Ansys-CFX 12, Lucino et al. [26] used Flow-3D with LES and Split Lagrange free surface tracking model, Bayeul-Laine et al. [27]used Star CCM+ V6.06 CFD with both SST k-ω and Realizable Two-Layer k-ε models as turbulence models and Hamed et al. [28]used Flow-3D with LES turbulence model. Hence, after the literature review Flow-3D CFD software was selected considering its user-friendly meshing methods, geometry defined methods and boundary condition defining flexibility.

3.1. Flow-3D CFD Software

Flow-3D is a CFD code developed by Flow Science Inc. The code simulates fluid dynamic models numerically by using Finite Volume Method, and based on solving Navier-Stokes equations. Further it is equipped with some other useful models, such as moving rigid bodies, flows in porous media, sediment transport, heat transfer, granular flow.

Modeling the free surface of the fluid is a key point of interest in this study. There are several free surface modeling methods used in CFD, such as: Interface tracking, Interface Capturing, Volume of Fluid (VOF) and Hybrid methods. Flow-3D uses the VOF method to compute free surface of a fluid. The technique was first identified by Hirt and Nichols [34].The method identified grid cells without fluid as fraction zero, with fluid as fraction one and partially filled cells as fraction in-between zero and one. VOF algorithm reduces the computer power requirement as it adds only one additional equation to the solver. Instead of computing the flow in both air and liquid

sections, VOF defines the air using the boundary condition of thin viscous boundary layer in-between air and water interface.

Flow-3Dsoftware package comes with a Graphical User Interface (GUI) with following tabs:

- **Simulation Manager:** Under Simulation Manager, user can manage and have access to simulation portfolios, interrupt simulations with new parameters, location of simulation files and online simulation process monitoring.

- **Model Setup:** Under this tab user can define the complete problem by using another six sub tabs as explained below:

    a. **General:** More general specifications of the problem are defined, such as the finishing time of the computation, interface tracking options, number of fluids involved, flow modes (whether it is compressible or incompressible) and units to be used throughout the problem.

    b. **Physics:** There are several physical models available for the user to define the problem with more flexibility. User should activate the models depending on the problem to be solved. Gravity and Non-Inertial Reference Frame, Viscosity and turbulence, density evaluation, surface tension, heat transfer, Air Entrainment and more generic models that can be activated.

    c. **Fluid:** Working fluids and their properties are defined under this tab.

d. **Meshing and Geometry:** User can create or import the geometry, define the computational domain with meshing, assign boundary conditions and initialize the problem under this tab. Flow-3D has its own 3D modeling option, or else user can import solid drawings directly to the working area in STL (Stereolithography) format. Software is also capable of defining history probes and mass sources as suitable to the fluid dynamic problem. Main advantage of the code is its ability to create hexahedral meshing, independent of the geometry of the model.

e. **Output:** Output tab controls the results files. User can select and manage required results depending on the requirements and the capacity of the computer. User can define restart data interval in case there is a need to restart the simulation after a previous usage.

f. **Numeric:** This is the last tab under the Model Setup. It defines the final stage of the model specifications. The specifications defining the numerical scheme to be used and its stability, are decided under this tab. Defining explicit or implicit methods, initial and minimum maximum time steps, VOF modeling method, Fluid flow solver options and momentum advection are the most important selections.

- **Analyze:** Method of analyzing the results is defined under this tab. Many kinds of plots such as 1-D, 2-D and 3-D are available for the user to define planes or volumes. Text file result are also a possible option, with an ability to obtain historical data at a defined point, and by using a Point Probe.

- **Display:** This is where a user can obtain graphical results as per the criteria selected under the Analyze Tab. Making of movies and taking snapshots of graphical results are also a possible option.

3.2. Hydraulic Model to validate the CFD code

In order to validate the CFD model, before applying it to the full-scale model, a scale down model was built by using Perspex and PVC. The scale down model is not geometrically similar to the actual intake and the reservoir. However, the functional characteristics are similar. The intake of the model is 32mm in diameter and protruded into the modeled pond with the pipe wall thickness of approximately 6mm. Water is circulated within the system using a centrifugal pump where outlet of the pump is directed back to the pond, in order to maintain specific water level of the pond. Considering financial limitations, a flow meter is not fixed, the flow rate is measured by using a Beaker. When compared to the quantity of the water in the pond, the level difference had negligible effect to the flow measurements. To minimize the waves within the physical model a Styrofoam obstacle is introduced in front of the intake and set close to the outlet of the pump. Dye is used to track the vortices easily. The actual arrangement of the model is shown in Figure 3-1. Solidworks 3D modeling software is used to model the pond and the intake. Figure 3-2. shows a view of a 3D model.

Figure 3- 1: Physical Model operating with a dye to track vortex formation

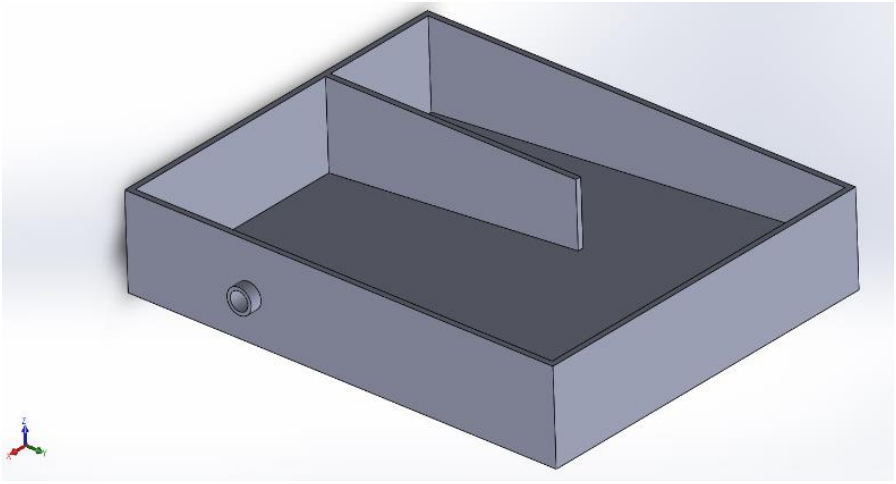

Figure 3- 2: Solid model of the test setup

During the physical model testing, steady type 06 vortex[6] is formed just above the intake at a flow rate of 0.65ltr/s and at a submergence of 40mm from the centerline of the intake pipe. Figure 3-3 represents the vortex formed with the assistance of dye.

Figure 3- 3: Air core type 06 Vortex formed in the physical model

The calculated Fr, Re,(h/D) and critical submergence (S) calculated as per the equations (32, 33) are given in the following table 3.1. S_a is the actual submergence presence.

Fr	Re	h/D	S (m)	Sa(m)
1.446 > 0.5	$2.9x10^4$	1.5	> 0.0224	0.024

Table 3- 1: Non-dimensional and critical submergence required an association with the state of the physical model.

3.2.1. Initial setup of the CFD Simulation of a physical Model

Setting up the CFD model is carried out with the 3D CAD model prepared by using Solidworks. Finish time is initially set to 50 seconds. The state of the other parameters is as follows:

Interface Tracking Method: *Free Surface*
Flow Model: *Incompressible/Limited Compressibility*
Number of Fluid: *One*
Turbulence Model: *As per the literature available, it is evident that the vortex was successfully modeled with Large Eddy Simulation (LES) turbulence model. Lucino et al. (2010) and Hamed et al. (2014). Hence, the turbulence model is selected as LES with No-Slip wall boundary condition.*
Surface Tension Model: *Based on the literature, the surface tension model is not activated. See section 2.3.2.*
Gravity: *Gravity is activated for the -Z direction as per the model reference coordinate system with a value of 9.81 m/s^2.*
Fluid: *Water at 20ºC with properties, Density 1000kg/m3 and viscosity 0.001kg/m/s is used.*

3.2.2. Meshing the computational domain:

The solid model, created by using Solidworks software, is imported directly to the workspace of Flow 3D with STL binary format. Correct reference coordinate frame and the units are the most important factors when creating the STL executable file by using Solidworks.

Meshing is the most important factor to be considered due to the small scale of the model. Flow 3Dprovides hexahedral type meshing, which can be introduced independently to the geometry of the solid model. This feature saves time in dealing with complex geometric meshing, and provides the user with the maximum flexibility and simplicity. The following factors are considered during meshing.

Computational Domain: The entire solid model is selected as the Computational domain to minimize the effects imposed from downstream and upstream boundary conditions.

Element size of the mesh (Grid size): This is the most challenging activity during meshing. The grid size shall be adequate enough to grab the vortex formation which is very small in geometric scale. In addition, it is intended to select the solver, based on the Explicit method considering advantages described under section 2.2.3. Hence, time step size highly depends on the selected element size in conjunction with the fluid flow velocity due to Courant Criterion. Courant number shall be less than 1 as explained in section 2.2.3. Furthermore, Flow 3D uses Fractional Area-Volume Obstacle Representation (FAVOR) algorithm to define the solid body. To capture the required features of the solid body the grid size should be adequately fine. Since the intake pipe is protruded into the tank and the thickness of the pipe is only 6mm, grid size of the surrounding area should be less than 3mm. Finally, increasing of grid size directly influences the solution time. Considering all these factors and after testing, several mesh sizes with following grid arrangement are finalized.

The ability to create smaller mesh block with finer mesh sizes in Flow 3D is of great help to make the required grid arrangement for the numerical model. These small mesh blocks are identified as “nested mesh blocks” in Flow 3D. Three mesh blocks are created with three different mesh sizes, 0.007m, 0.0035m and 0.00175m, respectively. The first mesh block covered the whole domain, and the other two covered a very small area, which is where the vortex is assumed to be formed. The intermediate mesh block is required to maintain the scale factor of 2 within two adjacent mesh elements and in order to fulfill the stability requirement of the CFD package. Figure 3.4. illustrates the final meshing arrangement of the model.

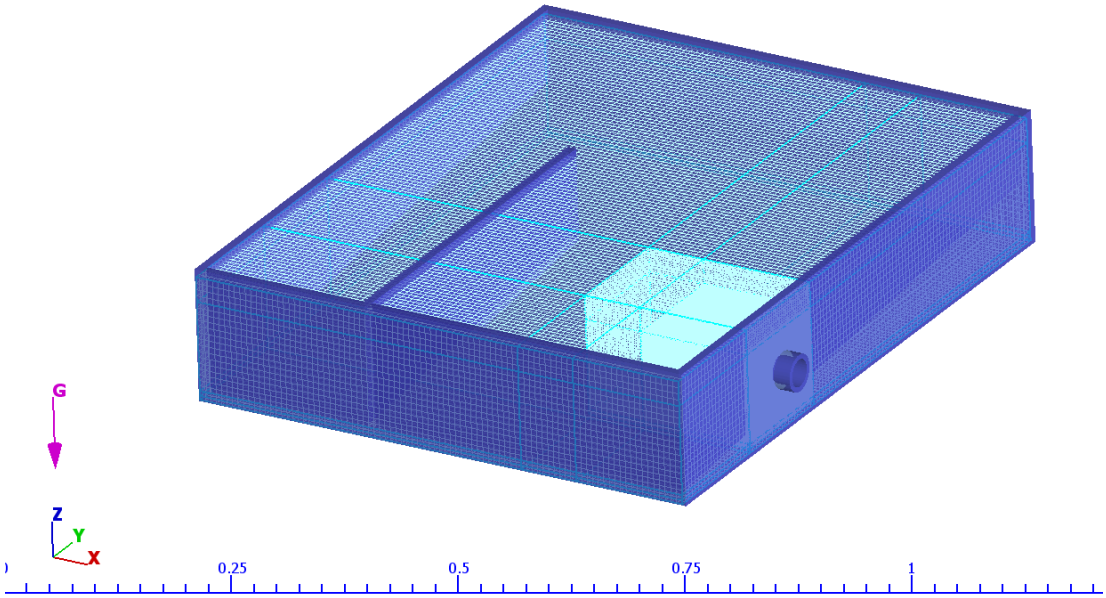

Figure 3- 4: The meshing arrangement of the model including two nested mesh blocks

The FAVOR function confirms the fully defined solid geometry and the space available for fluid with the created mesh. Mesh should be fine enough to grab the important geometry. The result after the FAVOR test is shown in Figure 3.5.

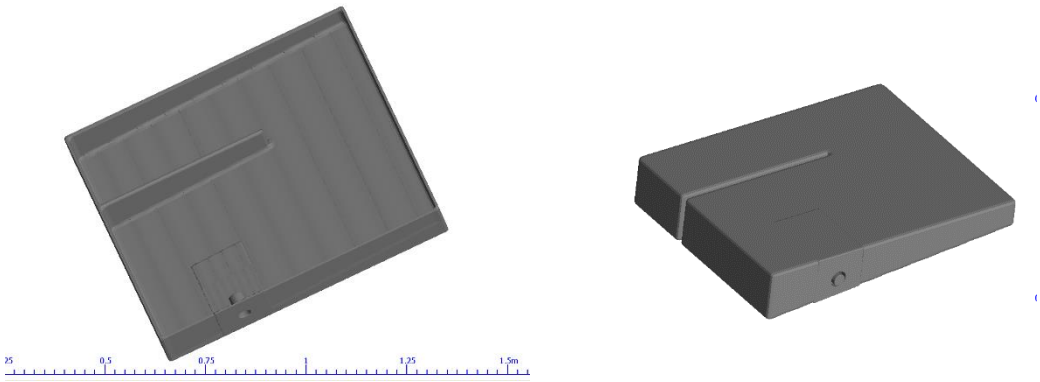

Figure 3- 5: Solid and Open volume after FAVOR algorithm. The left side is the solid volume and the right side is the open volume.

After defining the solid geometry and the mesh blocks boundary conditions are assigned to each and every face of the mesh block. All faces of the mesh blocks have to be defined with the boundary conditions. Boundary conditions are to be set so as to match with the actual condition of the physical model. The water level of the numerical model has to be maintained at a constant level while keeping the specific constant volume flow rate out.

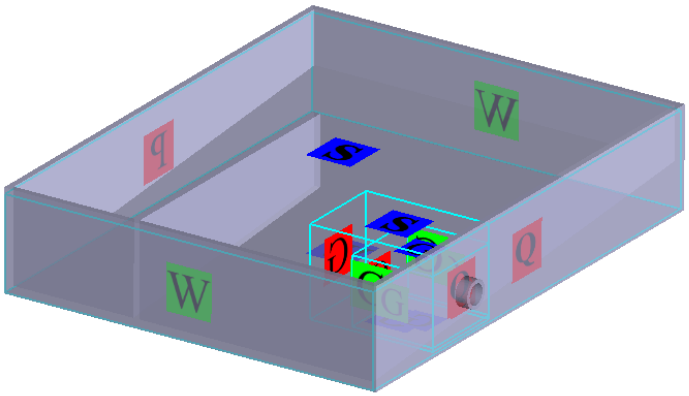

Figure 3- 6: Mesh planes and Boundary Conditions

These physical conditions are produced by setting the outlet side of the mesh face as Volume Flow Rate (Q), where the solver maintains constant flow rate through that boundary; the Opposite side of it, is set as Specific Pressure (P) and defined by the fluid elevation, where the fluid elevation is always a constant; the Topside face of the

block is set as Symmetry (S) boundary condition, where no fluid transfer in-between the plane is permitted and the velocity, normal to the symmetry boundary condition, is zero; the left, right and bottom sides of the mesh block are set as Wall (W) boundary condition, where the solver treats these faces as no slip solids. All the other faces of the nested blocks are set to Grid overlay (G) boundary condition, where the solver identifies them as inside of another mesh block. Figure 3.6. represents the numerical model with boundary conditions. Figure 3.6. Boundary conditions with grid lines of three meshing blocks.

3.2.3. Initialization of the Numerical Domain

Initialization is the condition of the numerical domain when time (t) is equal zero. The condition of the fluid regions inside the domain should be defined at t=0. The initial conditions of the present problem are the hydrostatic pressure of the fluid or the water level at t=0 instant. This has to be defined by modeling the water quantity inside the numerical domain by using Fluid Region creating option. Flow 3D identified the volume fraction of the defined fluid in a single fluid problem as 1, and the 0 represents the void region. Fully defined numerical model after initialization shown as Figure 3.7.

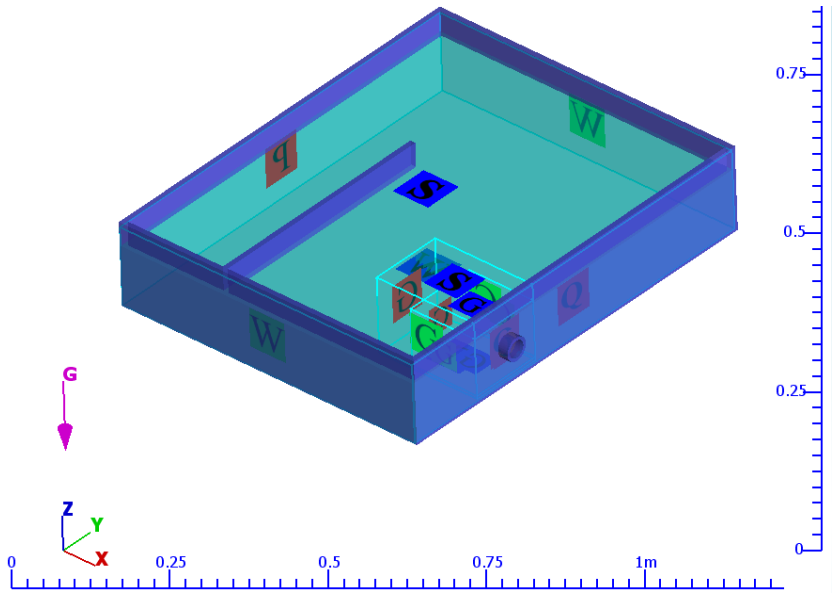

Figure 3.7: Fully defined numerical model after initialization

3.2.4. Simulating the numerical model

After developing the fully defined numerical model the simulation is started. The initial time interval is selected as 50s. Among the selections of numerical options, Split Lagrangian method is selected as the Volume of Fluid (VOF) advection method. Momentum Advection accuracy control method is selected as Second Order monotonicity-preserving. As per the user manual[35] of the software, the method is recommended to study swirling free surface flows. Momentum and the continuity Equations are selected as Fluid flow solver options. Since no energy transfer is considered in or out from the domain (isothermal), the energy equation is not solved.

The results of the numerical model are in good agreement with the physical model observations. Those results are discussed in the section 4.1.

3.3. Modeling the Samanala Intake

The actual scale solid model of the Horizontal type intake of the Samanala Power Station is prepared by using Solidworks software. The intake structure, including the concrete structure and the steel trash racks, is modeled to the exact dimensions, as per the construction drawings available with Laxapana Power Station's Drawings Library. Figure 3.8. illustrates a final solid model of the intake structure. The intake structure has three openings, same in size with inclination in its horizontal plane. The intake was constructed roughly in 1966. At the time, no extensive literature and studying techniques and formulas, were available regarding the free surface vortices.

Modeling of the reservoir (Pond) is a challenging task. No original contour map of the pond is available. However, a contour map, which was surveyed in 1987 by National Hydrographic Office of National Aquatic Resources Agency (NARA) [36], is available. For the simplicity of the hydraulic model, only the dam and the right abutment slope (when facing from the dam) where the intake is situated, are modeled

using Solidworks. The final solid model, prepared for the numerical simulation works with the intake structure, is shown in Figure 3.9.

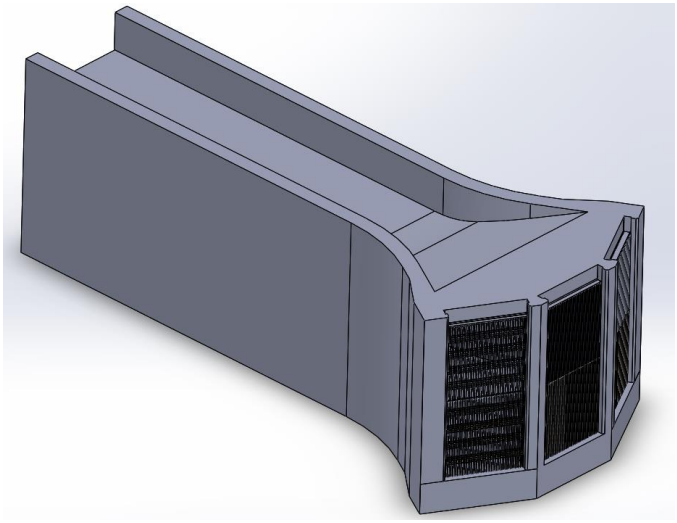

Figure 3- 8:Isometric view of the solid model of the Intake structure

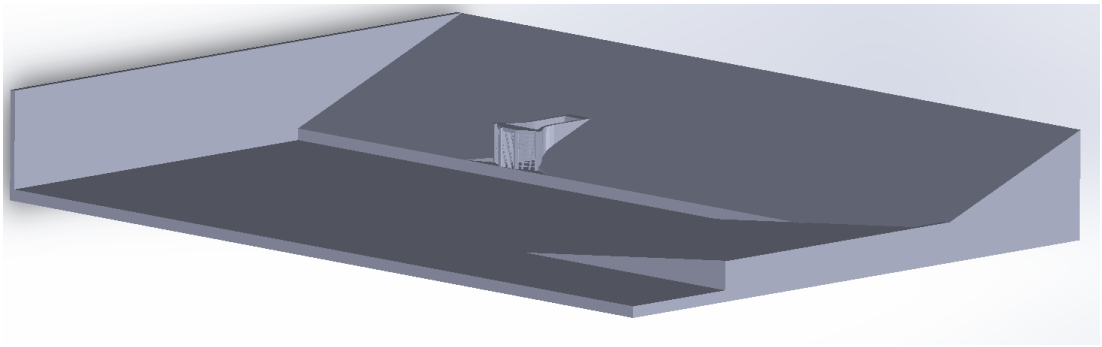

Figure 3- 9: The final solid model including the intake structure

3.3.1. Numerical simulation setup

The initial setup for the CFD simulation for the actual model is the same as the physical model simulation setup. The only difference is the meshing. Since the velocity associated with the domain is in the same scale as it is in the physical model and the vortex to be observed is large enough to be modeled using a coarser mesh, the Courant Criterion can be easily met. However, the difficult task is capturing the trash rack with the FAVOR algorithm. Since the trash rack profile has 6mm thick flat bars, the mesh around the trash rack should be at least within 2 to 3 mm range, which is not possible, as it increases the total number of mesh cells enormously. Hence, taking into consideration the available computer power and the time taken for such a simulation with large number of cells, studying the effect of the trash rack to free surface vortex is not carried out during this study. Only the intake structure is considered without the trash racks.

Meshing: Two mesh blocks are made with 0.4m coarser mesh and 0.2m finer mesh. The coarser mesh covers the whole domain, while the finer mesh covers only the approximate interest area, where the vortex was physically observed during the operation of the power plant. The height of both the mesh blocks is set to 3.5m, from the top deck of the intake, which is adequately higher than the calculated minimum submergence at full flow of 36.4m^3/s, as per the equations 30 and 31.

$\boldsymbol{Fr}$	$\boldsymbol{Re}$	S (m)
0.39< 0.5	1.2x10^7	> 2.975

Table 3- 2: Non-dimensional numbers for Samanala Intake at Full Flow

Following table 3.3. summarizes the mesh block information:

Mesh Blocks	Number of Cells
Main Mesh Block (Coarser Mesh – Cell Size 0.4m)	2,073,762
Second Mesh block (Nested Block with Fine Mesh – Cell Size 0.2m)	850,000

Table 3- 3: Mesh block information of the numerical model of actual intake structure

Before arriving to the above cell sizes, combination of 0.5m and 0.25m cell sizes was tested. However, no favorable results have been obtained during the expected time duration. Further reduction, to less than 0.4m and 0.2m, is not considered, due to the limitation of the computer power and the time. Furthermore, FAVOR algorithm successfully accessed the required solid boundaries. Boundary conditions were the same as they were in the physical model. Solid model, after the FAVOR function and setting up boundary condition with mesh blocks, is shown in Figure 3.10.

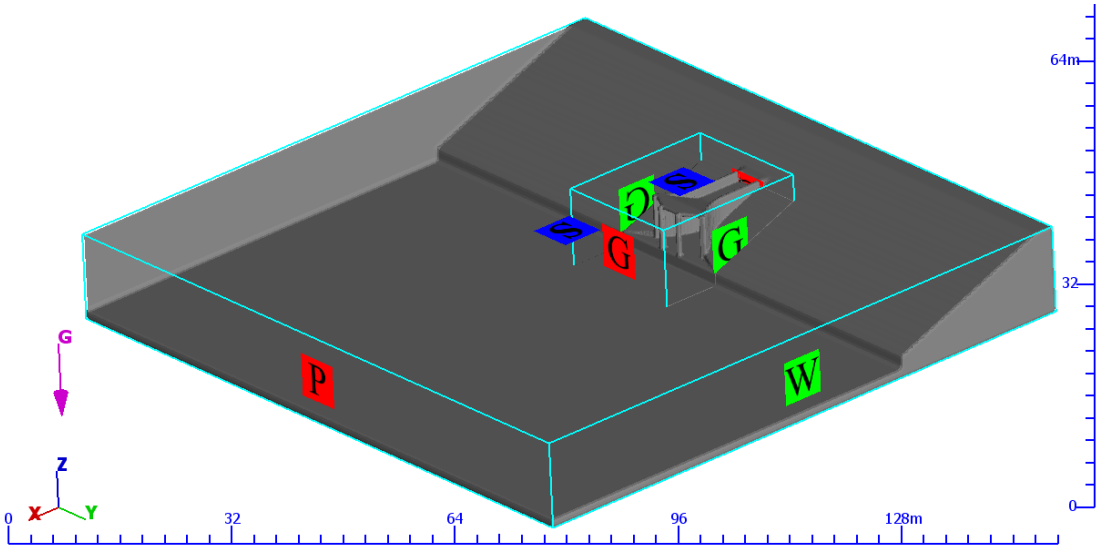

Figure 3- 10: Result of FAVOR algorithm for mesh size evaluation for the Solid body including boundary conditions and mesh blocks

Figure 3.11. provides a better understanding about the nested mesh blocks with denser mesh cells.

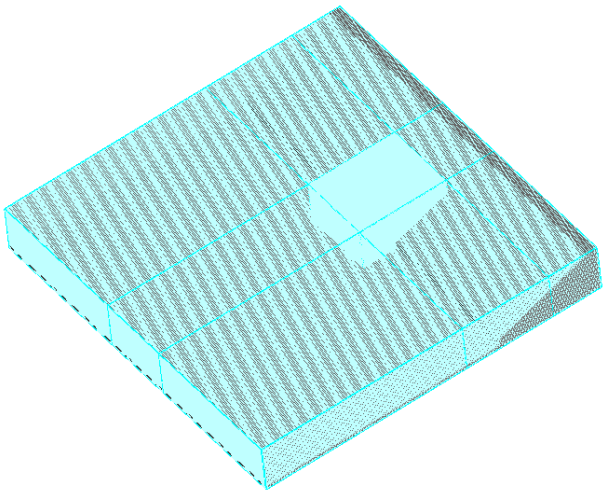

Figure 3- 11: Nested mesh arrangement of the numerical model

3.3.2. Numerical Simulation of the actual intake model

After setting up the numerical model, the model is ready to run the required simulations with different conditions. Initial attempt is to check the critical submergence level for the intake structure. For the identification of the component, coordinate system is used as illustrated in Figure 3.10. The origin of the coordinate system is shown in Figure 3.12.

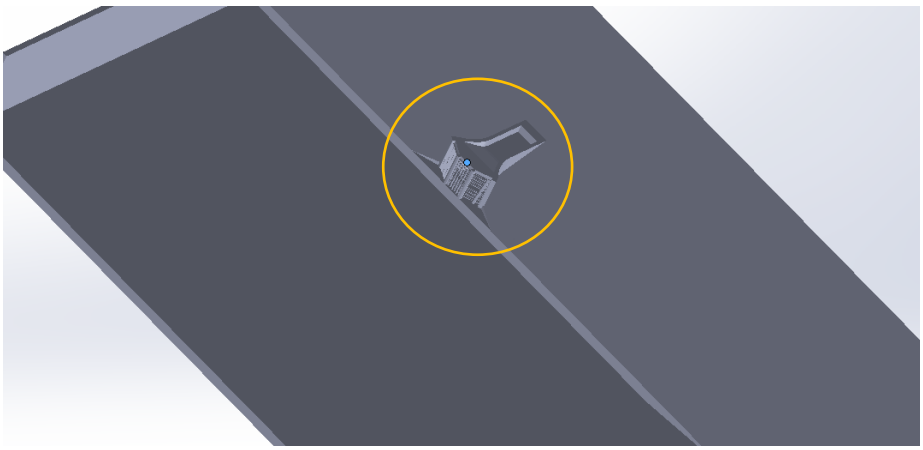

Figure 3.12: The origin of the Solid model (Blue Dot)

As per the coordinate system, -X side is where the flow goes in towards the tunnel, the +X is the right abutment, when facing from the Dam, -Y side is where the Dam is situated, while +Y is the distance that is to be varied during the simulations, in order to provide eccentric flow approach conditions to the intake, -Z side is where the gravitational force is applied, and +Z is the top surface of the computational domain, which is the atmosphere. This notation is used while explaining the results of the simulations.

CHAPTER 4. RESULTS AND DISCUSSION

4.1. Numerical Code Validation Results

Results obtained during the validation of the numerical model are discussed in this section. Comparison between numerical model and the physical model is used to verify and analyze the findings. Deficiencies introduced due to the nature of the numerical model will also be discussed here.MS Excel and “FlowSight” software package, which is from the same developer as Flow-3D, are used to interpret the results.

4.1.1. Challenges to be overcome during the validation process

Prepared numerical model has limitations in setting up the computational mesh as discussed in the section 3.2.3. As explained in the sections 3.2.3 and 2.2.3. Courant Criterion is limiting the time step size from increasing up to higher values, which in turn drastically increases the time taken for the simulation process. Available computational resources for this study were not sufficient to carry out the complete calculation. Hence, simulation is run for a sufficient time duration until the initial vortex is formed.

4.1.2. Comparison of Physical and Numerical model

Due to the reason explained in the section 4.1.1. the simulation was stopped after 7 seconds (Physical time), which was sufficient for starting of whirling motion at the expected region and to check the vortex structure details for the comparison. Figure 4.1. illustrates the vortex core generated during the simulation just above the intake pipe, and very close to the place where the vortex appeared in physical model testing. A strong type 6 vortex (Alden Research Laboratory, MA, U.S.A. (ARL) [6]is formed in the physical model, in very close proximity to the vortex generated by the numerical model. Refer to Figures 3.1 and 3.3 for the physical model results. Furthermore, this result is in good agreement with the experimental and numerical results obtained by Hamed et al. [28]using same type of simulation. The only

difference of the test is the size of the intake pipe and the Fr number. The study of Hamed et al. [28]has been carried out for Fr 1.2 maximum, while the present study has Fr at approximately 1.4.

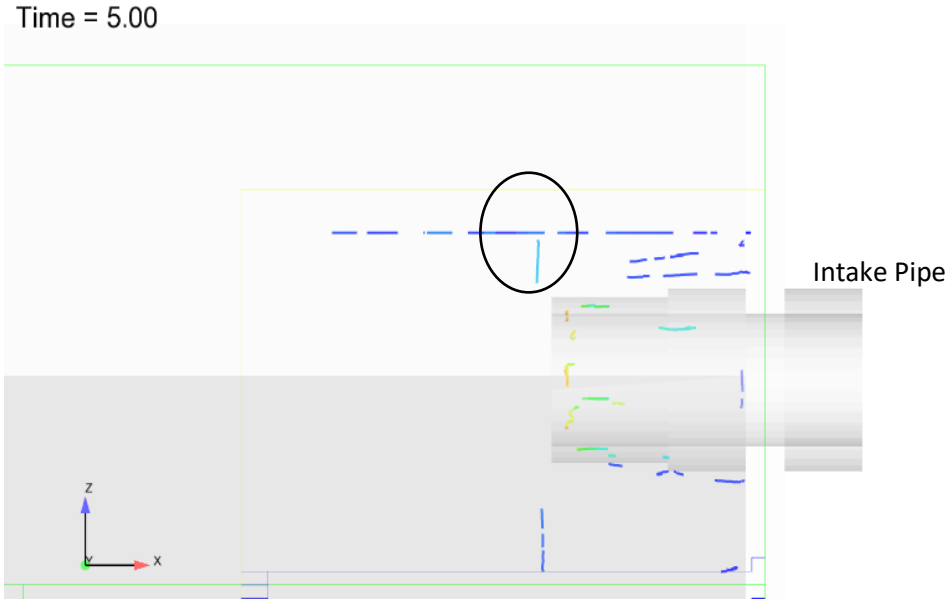

Figure 4- 1: Vortex core representation of the numerical model of the Physical model (Time = 5s)

Streamlines starting from a plane parallel to the free surface of the water surface were also generated to identify the structure of the vortex. Figure 4.2. and 4.3 illustrates the velocity vector and streamline representations of the vortex. The approximate diameter of the vortex at the free surface is about 30mm, which is, also approximately, the same in size with the physical model. The swirling motion on the surface is well represented, however, the vortex core to the intake is not sufficiently developed due to the limitation explained in the section 4.1.1.

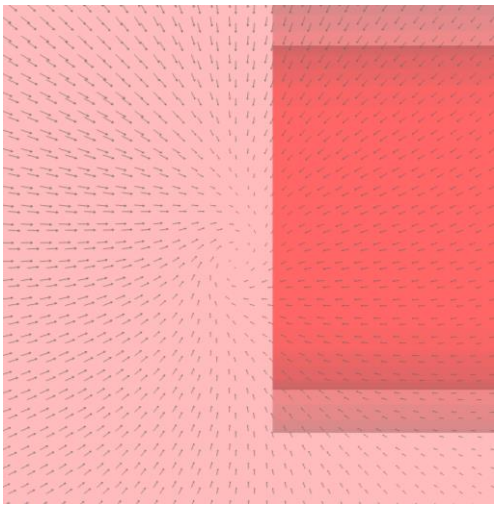

Figure 4- 2:Velocity vectors of the vortex shown from the top of the intake

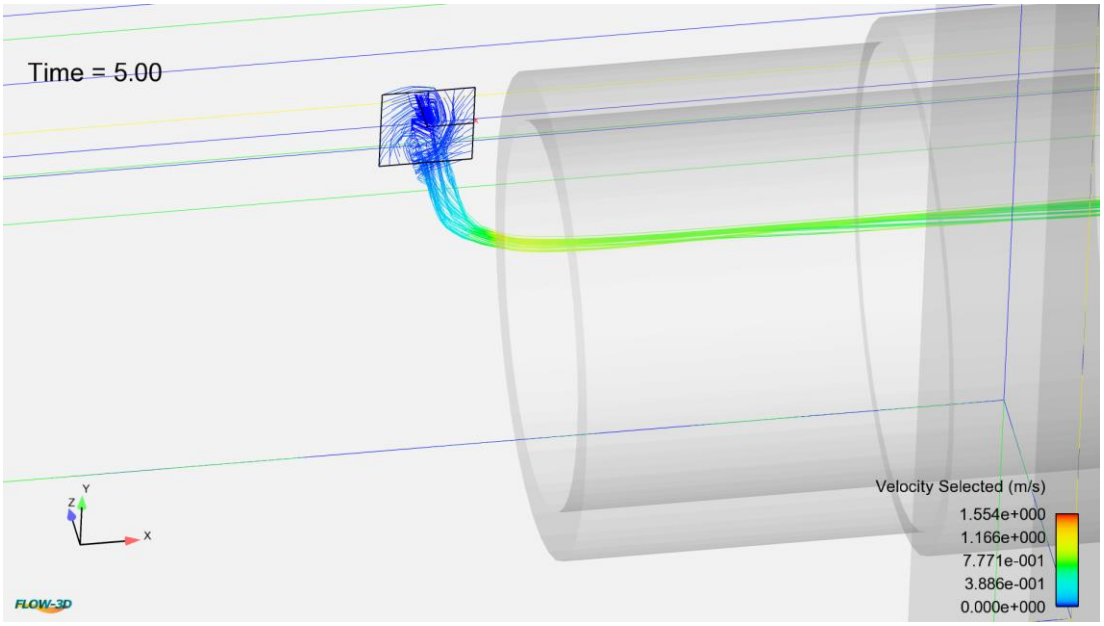

Figure 4- 3: 3D view of the vortex

To confirm the structure of the vortex, the y direction velocity distribution is plotted through a horizontal line which passes through the approximate center of the vortex perpendicular to the y axis. The coordinate system is shown clearly in figure 4.3. This velocity distribution is in good agreement with the Rankine [5] vortex model

theory. The velocity increases initially and decreases at the center point of the vortex, where forced and free vortex regions can be clearly identified as explained in figure 2.5. Figure 4.4. illustrates the plot of the tangential velocity distribution perpendicular to the y direction through the vortex.

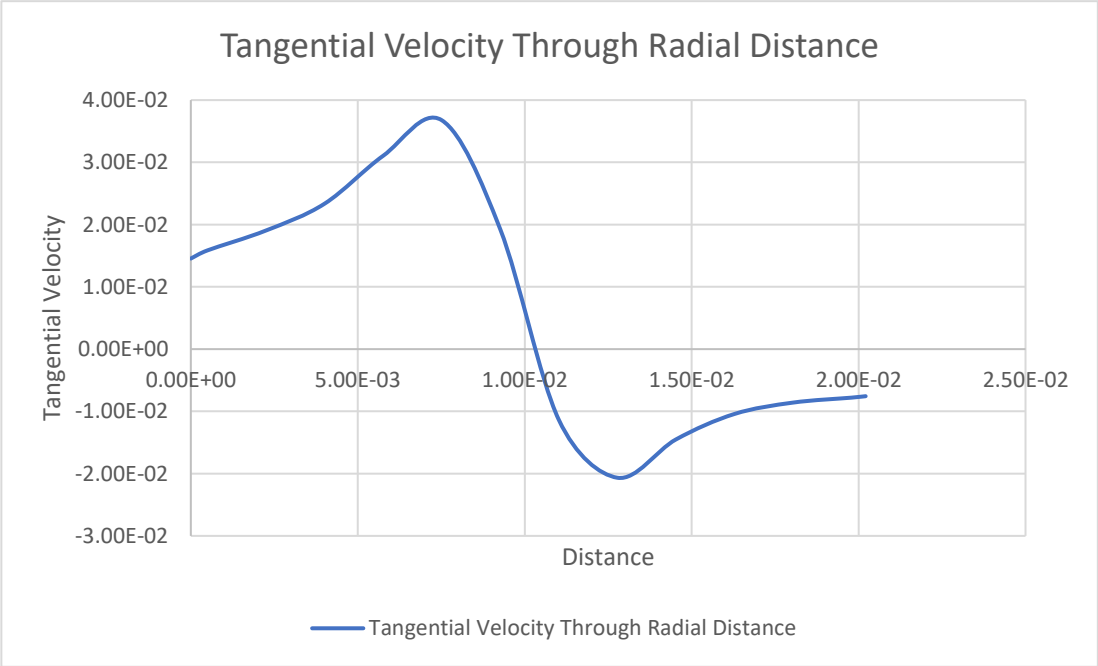

Figure 4- 4: Tangential velocity distribution perpendicular to the Y direction through the vortex.

As explained above the numerical model is suitable to identify the free surface vortices at protruded horizontal water intakes, same as in the Samanala Hydropower Intake structure.

4.2. Results pertaining to the simulation of Samanala Hydropower Intake Structure

Results of different simulations carried out for different conditions of Samanala intake structure, and by using a validated numerical model under section 4.2.1, will be discussed under this section. Critical dimensions of the intake, such as the minimum submergence, are required to calculate the intake Fr number at full flow and Reynolds number at full flow inside the intake conduit. Fr and Re are calculated

according to the equations 20, 21, 32, 33 and 35. Resulting values are given in Table 4.1. and figure 4.5. show the characteristic dimensions of the intake of Samanala Power Station. All the simulations are carried out for the maximum flow of 36.4 m3/s of the two hydropower Units of Samanala Power station.

Minimum submergence required	**Intake Fr number at full flow**	**Intake averaged velocity at full load**	**Reynolds number at full flow inside the conduit**	**Height of the intake conduit**	**Hydraulic diameter of the intake conduit**
6.36 m (eqn. 33) 5.09 m (eqn 30)	0.4	2.58 m/s	$1.23x10^7$	4.57m	4.24 m

Table 4- 1: Important dimensions of the Samanala Intake

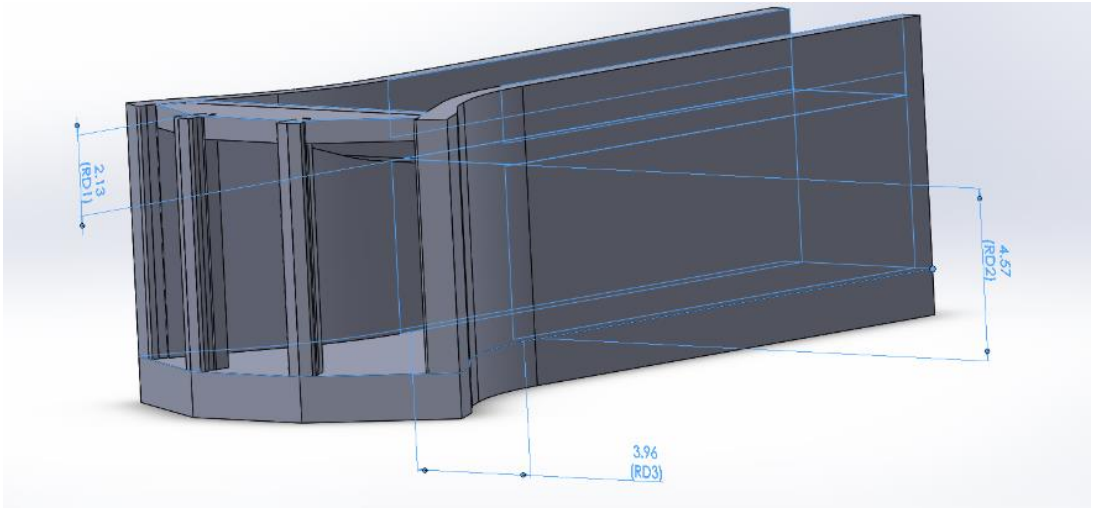

Figure 4- 5: Characteristic dimensions of the intake work of Samanala Power Station

4.2.1. The investigation of the vortex structure with the Submergence of the Intake

Study on the vortex formation with the submergence of the intake is carried out by a set of numerical simulations, with the model explained in section 3.3. In order to provide the actual flow model, as in the Samanala Intake, the computational domain is selected so that the intake is eccentrically situated, maintaining the constant distance to the dam, and similar to the actual value of approximately 50m. The intake blockage ratio is assumed to be zero. Following table summarizes the simulations carried out. The distances are measured as per the coordinate system described under the section 3.3.3., water elevation is defined as the initial condition of the model. S/D values are defined using the hydraulic diameter of the intake conduit. Run time for all the simulations is 100s. Solution is assumed to be steady after the automatic generation of the message by the software. The time step is controlled by the software itself.

Number	**S/D**	**Distance to the -Y side**	**Distance to the +Y side**	**Distance to the +X side**	**Water level elevation from the intake deck**
S1	0.89	50m	30m	68m	-0.6m
S2	1.03	50m	30m	68m	-0.01m
S3	1.15	50m	30m	68m	0.5m
S4	1.27	50m	30m	68m	1.0m
S5	1.4	50m	30m	68m	1.5m
S6	1.5	50m	30m	68m	2.0m
S7	1.63	50m	30m	68m	2.5m
S8	1.74	50m	30m	68m	3.0m

Table 4- 2:Domain setup for the different intake submergence simulations.

It was noted that, free surface vortices appeared in five of the simulations that were carried out, where S/D values are 1.15, 1.27, 1.4, 1.5 and 1.63. No free surface vortices are formed in the other simulations. Furthermore, no vortex is formed representing the water surface depression. To investigate the properties of the vortices, tangential velocities through the radial distance of the vortex structure and the vorticity are plotted. The approximate center of the vortex is identified by plotting the Vorticity of the flow field on a 2D cut plane through the Z axis, at a point closer to the free surface and generating vortex core reigns. Further plotting of velocity vectors helped to verify the circular motion of the flow. S4, S5 and S7 simulations confirm two distinct vortices and S3 and S6 give only one vortex. The velocity vector representation of the horizontal plane of the simulation S7 is shown in figure 4.6

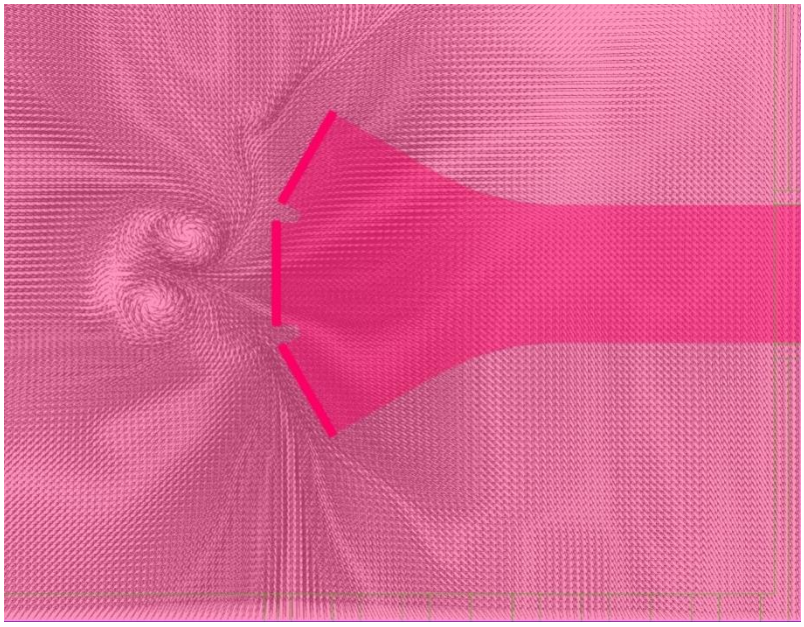

Figure 4.6: Velocity Vector representation of the flow field

Strength of free surface vortex formed in S5 and S7 reached its maximum at the end of the simulations. S3, S4 and S6 simulations show unstable vortices which appeared intermittently. The vortex appearing time of the simulations is given in the Table 4-3.

S/D values for simulations	Time taken to form free surface vortex
1.15 (S3)	40s
1.27 (S4)	40s
1.4 (S5)	100s
1.5 (S6)	93s
1.63 (s7)	100s

Table 4- 3: Vortex appearing time for each simulation

The tangential velocity and vorticity measurements are obtained using a 2D section plane through the Y axis, intersecting the identified center of the vortex. Measurements are taken along the line drawn through the vortex at a direction of X axis closer to the free surface. The 2D vorticity plots of S7 and S5 simulation, representing two vortices, are shown in figures 4.7. and 4.8.

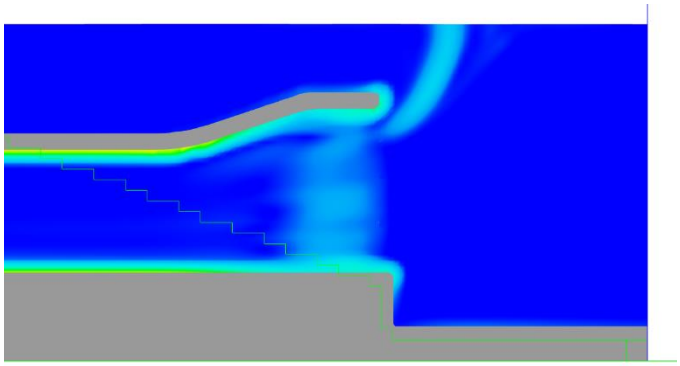

Figure 4- 7: Vorticity plot representing the free surface vortex structure (S/D=1.63)

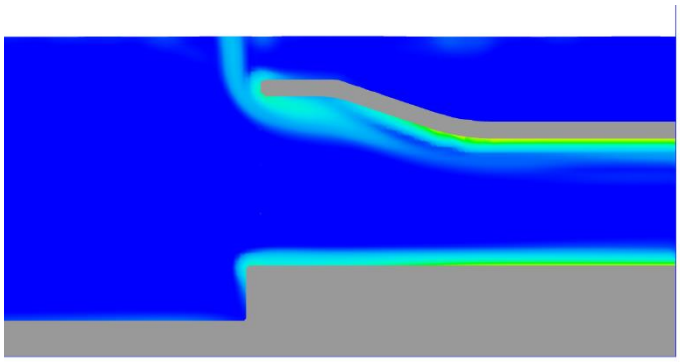

Figure 4- 8: Vorticity plot representing the free surface vortex structure (S/D=1.5)

Identification of the type of free surface vortices formed

Intention of this is to identify the similarities of the well-known free surface model introduced by Rankine (1858). Since the velocity measurements are taken along the X axis though the approximate center of the vortex, it can be assumed that the velocity measurements are taken perpendicular to the X axis, as tangential velocity component along the radius of the vortex. Hence, the Y velocity component is plotted against a radial distance through the vortex formed in all simulations. Figure 4-9. represents the tangential velocity distribution (Y velocity component along the X axis through the center of the vortex) and the vorticity distribution of the vortex structure along its radius, in simulation S7. Velocity and Vorticity values are divided by modulus of their highest value to take both parameters to be in between -1 to +1. Figure 4-10 illustrates the comparison of tangential velocity distribution along the diameter of the vortices, formed in all the simulations. Variation of tangential velocities of all the vortices first increases and then decreases. This pattern is well in agreement with the vortex model explained by Rankine (1858). Furthermore, this velocity distribution is in good agreement with the compound vortex explanation in Fluid Mechanics, John F. Douglas, (209). Two velocity distribution regions can be clearly identified by matching the free vortex region in the outer circle and forced

vortex region in the middle. Hence, it is evident that compound type free surface vortices are formed in all the above simulations.

As per figure 4.6 and figure 4.10, it is evident that in most scenarios two vortices are formed. Furthermore, they are in opposite rotational directions. For S/D values of 1.27, 1.4, 1.63 two vortices are formed in opposite directions, as such for vortices formed in a selected S/D value. Tangential velocity distributions span from negative to positive for a vortex, while from positive to negative in the other. There is no evidence that the S/D values are influenced by the double vortex formation.

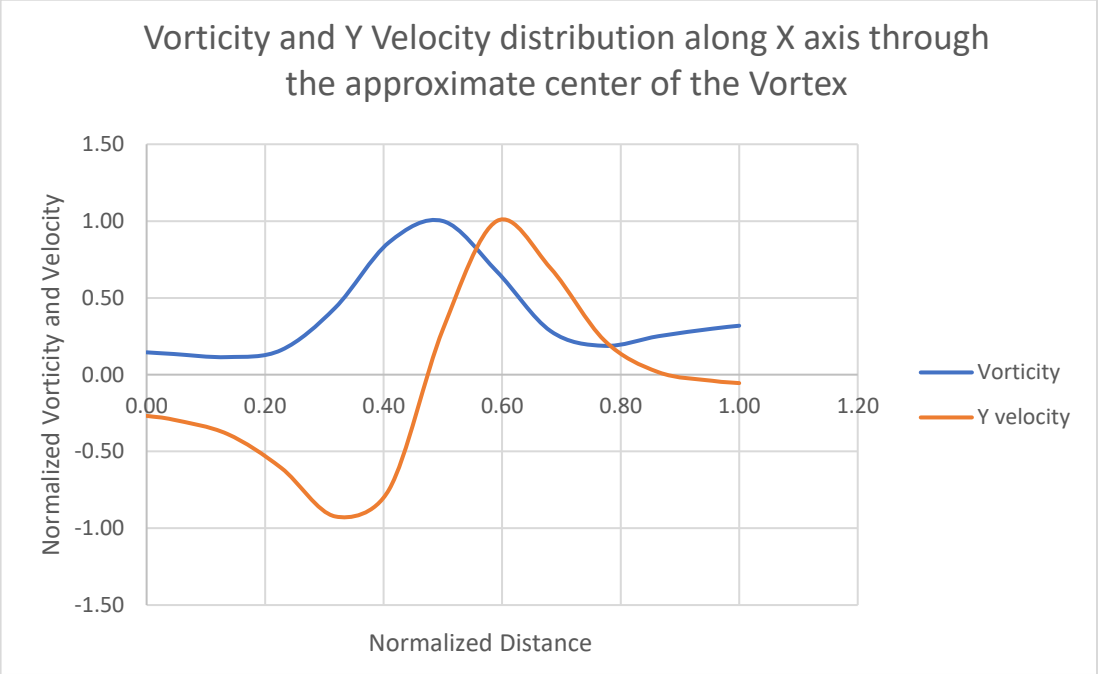

Figure 4. 9: Vorticity and Tangential Velocity (Y Velocity component) distribution along the X axis through the approximate center of the Vortex (S/D=1.5)

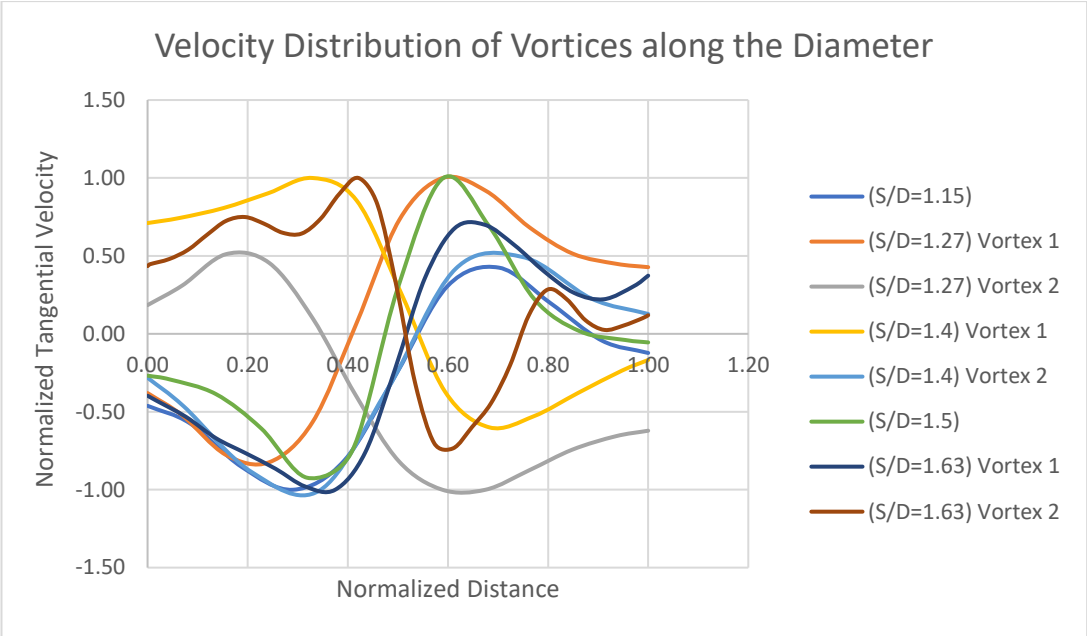

Figure 4- 10: Tangential Velocity distribution of all vortices along the diameter

Characterizing the origin location of the vortices

The location where the vortex originates is an important factor in designing anti-vortex structures. It will provide a good idea about the existence of the dead zone explained in Hamed et al. [28], which is due to the funnel shape flow in to the intake and the stronger shear layer between the flow and the water column close to the top of the intake. Figure 4-11. and figure 4-12. illustrate how the vortex positions are distributed with the different submergence levels. The x and y values taken from the approximate center of the vortex are plotted against S/D values in figure 4-11.,in order to investigate the position of the vortex formed with respect to the topmost face of the intake. The exact positions of the vortices with the distance to the centers, from the center line of the intake (as defined in section 3.3.3.), are plotted in figure 4-12. This figure will be used to investigate the vortex position distribution with the increasing submergence level. Forming of free surface vortices always happened in the positive side of the X direction, which means that the free surface vortices are always formed in front of the intake. No vortices are identified, with the position

behind the top most face of the intake. Furthermore, formation of two opposite direction vortices always happens in the negative and positive side of the intake centerline. Additionally, it is evident that, with the increasing submergence level, the formation of vortices is going further away from the intake structure to its front side (+ X side) and the formatted two opposite rotational vortices are further apart from each other. This means that the applicable dead zone increases with the submergence level. However, increasing of the dead zone does not increase the strength of the vortex formed. Strength of the vortex is discussed under the next paragraph "Strength of the Vortices".

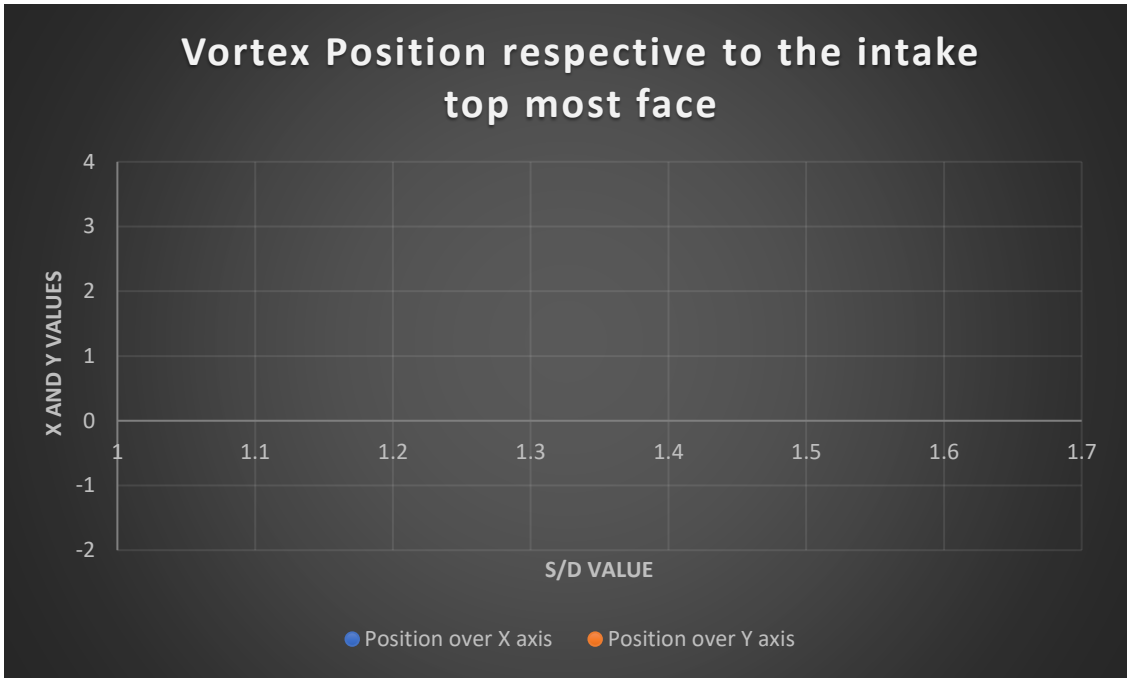

Figure 4.11: The x and y values taken from the approximate center of the vortices

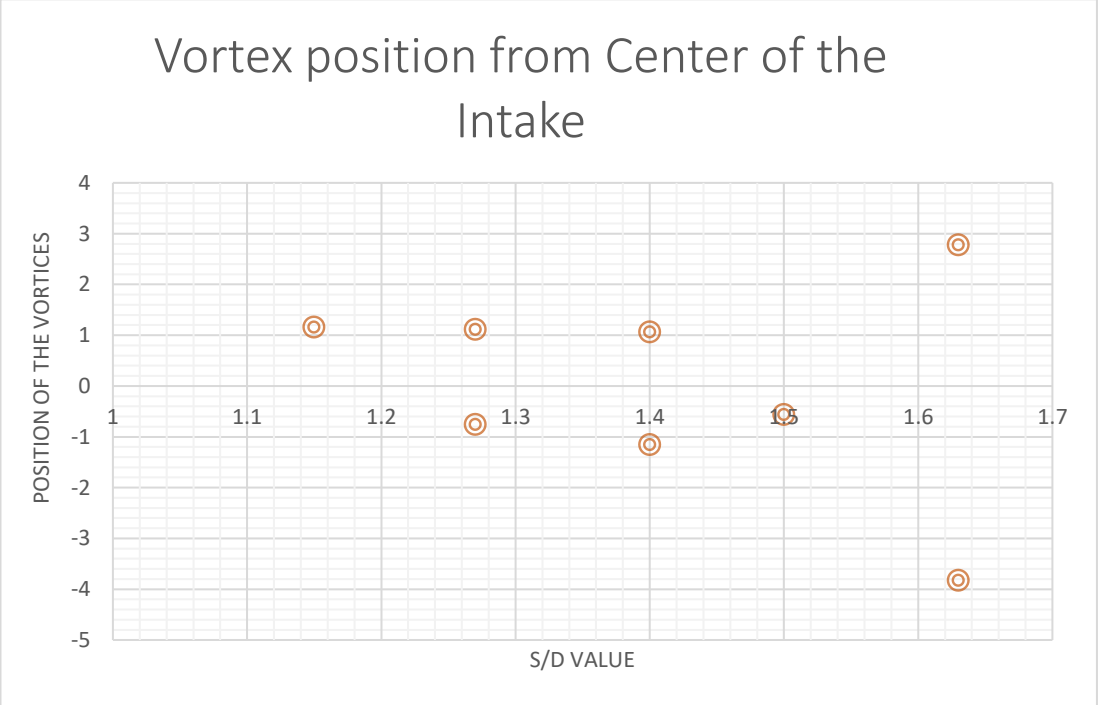

Figure 4.12: The exact position of the vortices with the distance to the centers of the vortices

Strength of the Vortices:

Strength of the vortices is investigated by comparing the tangential velocities, diameter of the vortices formed and the vorticity distribution along the diameter of the vortex structure. Figure 4-13 illustrates the vorticity distribution of all the vortices formed during the simulations respective to the S/D values. Vorticity is plotted against the normalized radial distance of the vortices to compare the vorticity in the same length scale. Figure 4-14 shows the diameters of the vortices formed, respective to the S/D values, and Figure 4-15 describes the tangential velocity distributions of the vortex structures over S/D values. Except the S6 simulation, the results show that the intensity of the vorticity decreases with the increasing of the submergence, while vorticity levels of 1.27 and 1.4 S/D values are approximately equal. However, the vorticity decreases with the increasing submergence. The

diameter of the vortices also tends to increase with the increasing submergence level. Magnitudes of the tangential velocities also decreases with the increasing submergence level. Hence, it is evident that the vortex strength reduces with the submergence level, even though the dead zone is increased, as explained previously. As Knauss [5] and Wu [12] explained, the inertia of the water column might be the reason for decreasing of the vorticity.

Furthermore, it is identified that the formation of vortices in lesser submergence levels is quicker than the higher submergence levels. Figure 4-16., figure 4-17 and figure 4-18. illustrate vorticity and the velocity distributions of a point inside the vortices, formed on different submergence levels. The velocity at the point first increases and oscillates, reducing its strength with time. The highest vorticity is achieved when the amplitude of the oscillated velocity wave form is smaller. Then the vorticity drops quickly, while the velocity is again increased and starts oscillating. The same cycle may continue if the simulation runs further, since the plots have more or less the same trends. This pattern further described the creation of the dead zone near the intake, as decreasing flow velocity and oscillating velocity field trigger the swirling motion.

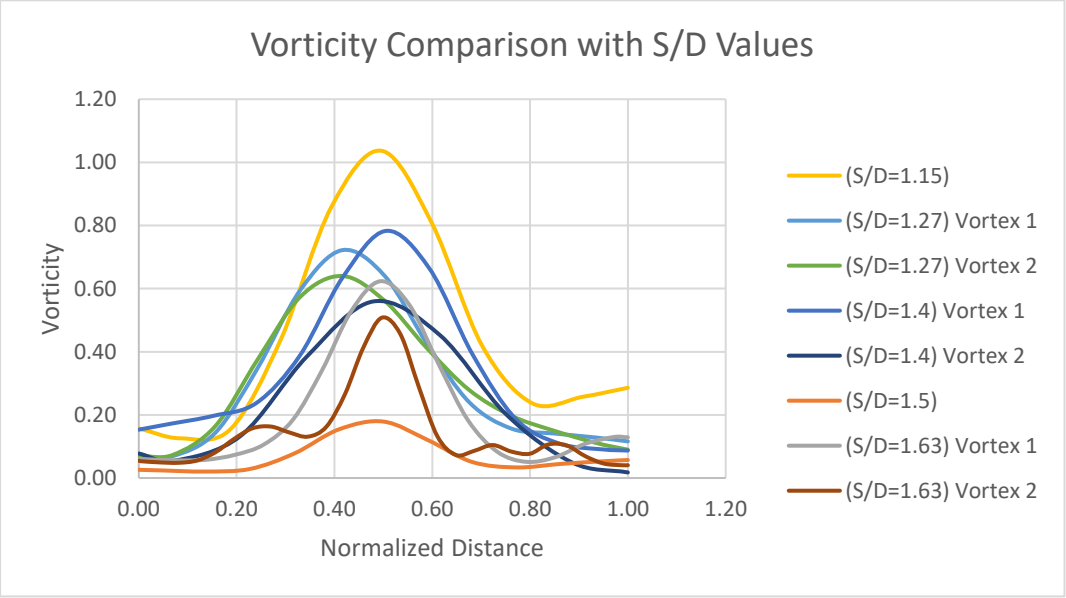

Figure 4.13:Vorticity distribution of all the vortices formed during the simulations respective to the S/D values.

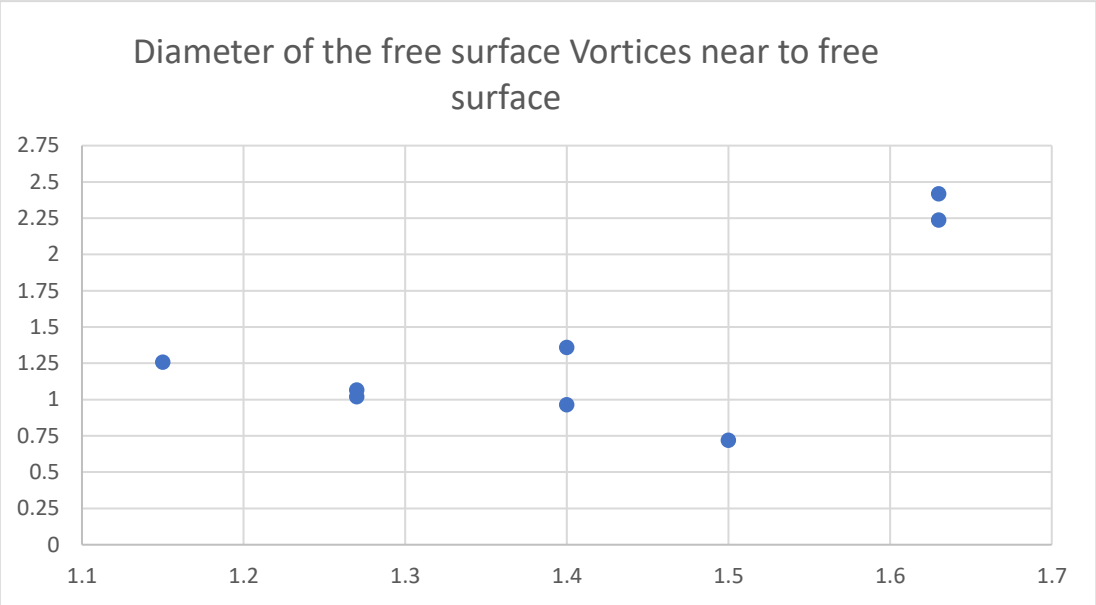

Figure 4- 14:Diameters of the vortices formed respective to the S/D values

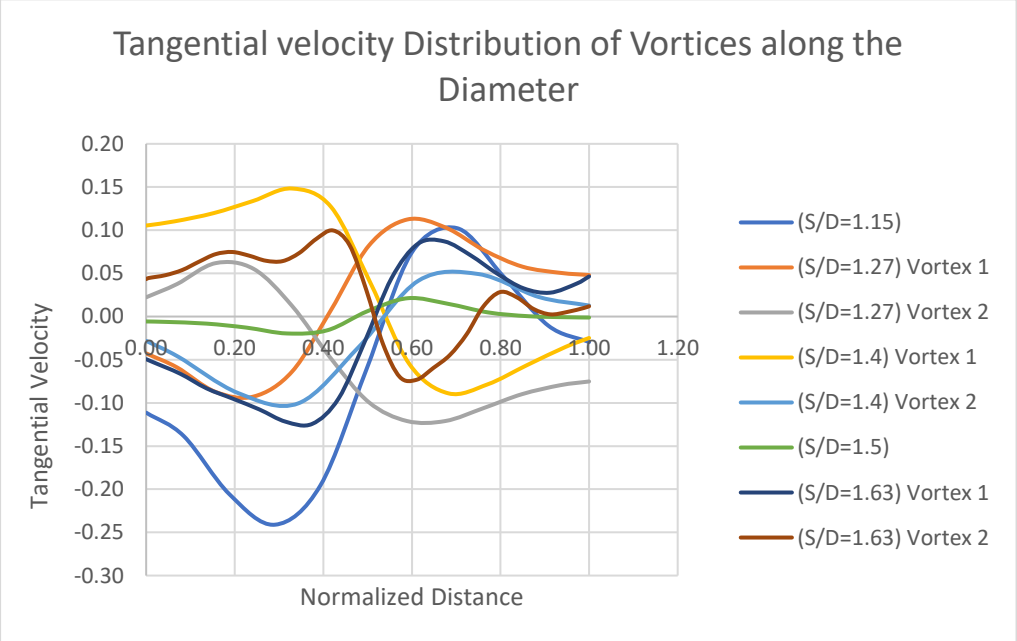

Figure 4- 15: Tangential velocity distribution along the radial distance of vortices

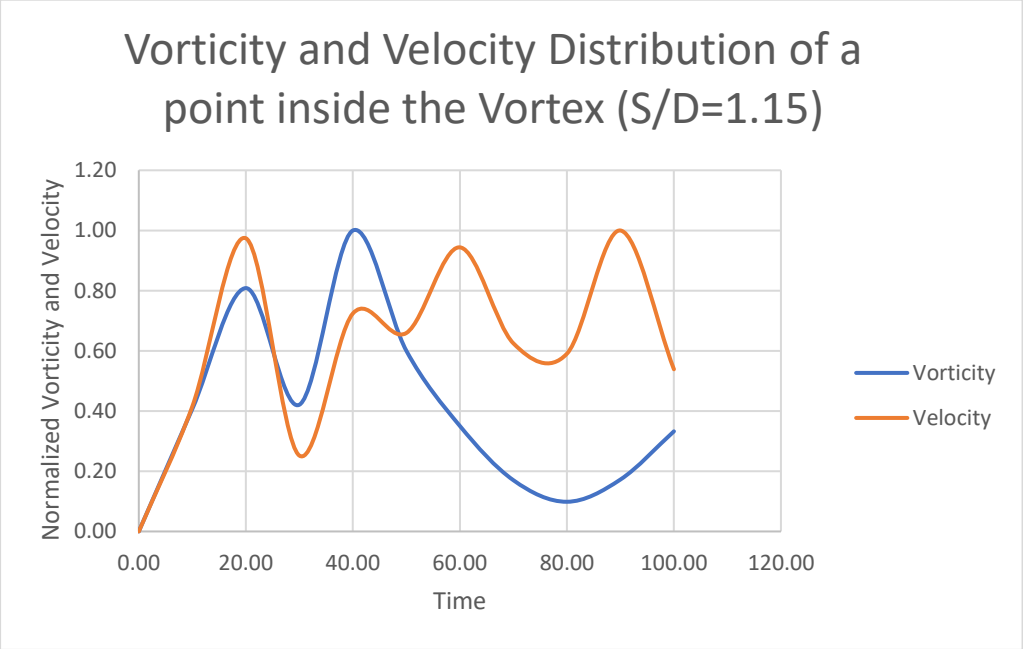

Figure 4- 16: Vorticity and Velocity distribution of a point inside the vortex (S/D=1.15)

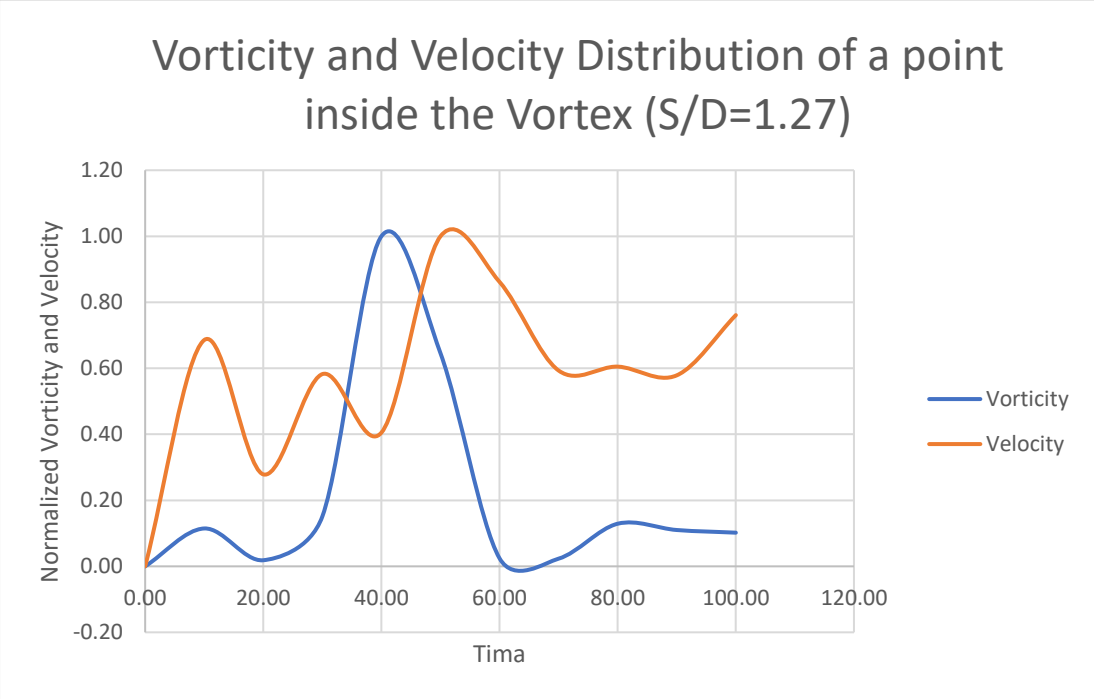

Figure 4- 17: Vorticity and Velocity distribution of a point inside the vortex (S/D=1.27)

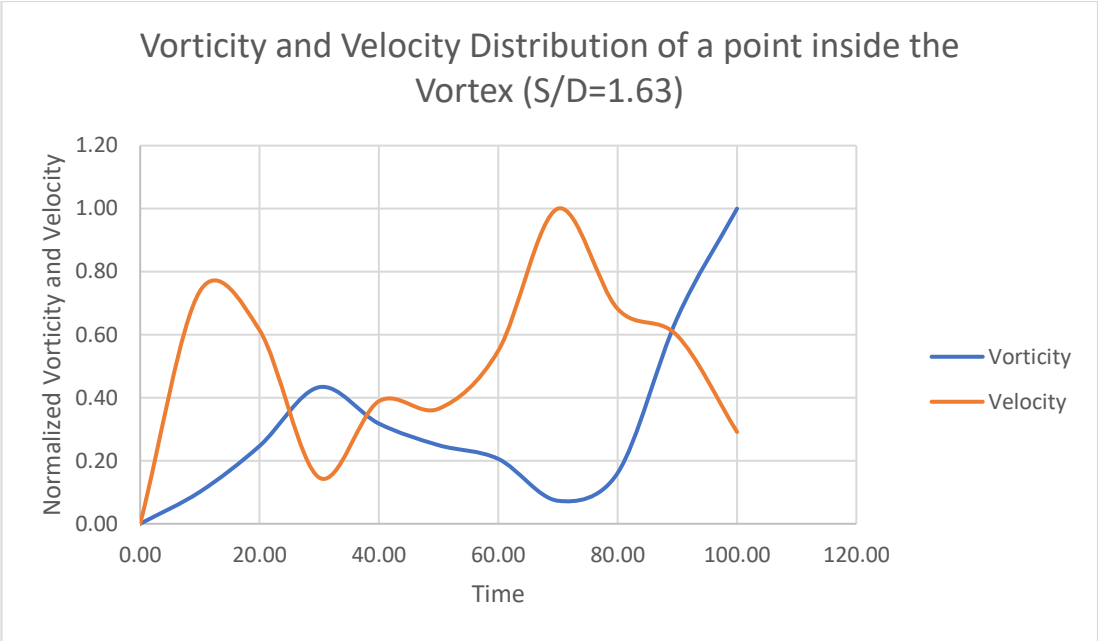

Figure 4- 18: Vorticity and Velocity distribution of a point inside the vortex (S/D=1.63)

Comparing vortex pairs, formed during simulations:

In all the simulations two vortices appeared and the rotational directions of the vortices were opposite to each other. It can be easily recognized by using the velocity vector representation in figure 4-6 and the tangential velocity distributions, in a radial distance of both vortices. Figure 4-19 illustrates the tangential velocity distributions along the radial distance, in the vortices formed during submergence level of S/D=1.63. Figure 4-20 shows the vorticity distribution of the same submergence level along the radial distance. As shown, one vortex is always dominating with higher vorticity in the other simulations as well. Furthermore, the vortex is formed in the -Y side, if the intake is always having the highest vorticity.

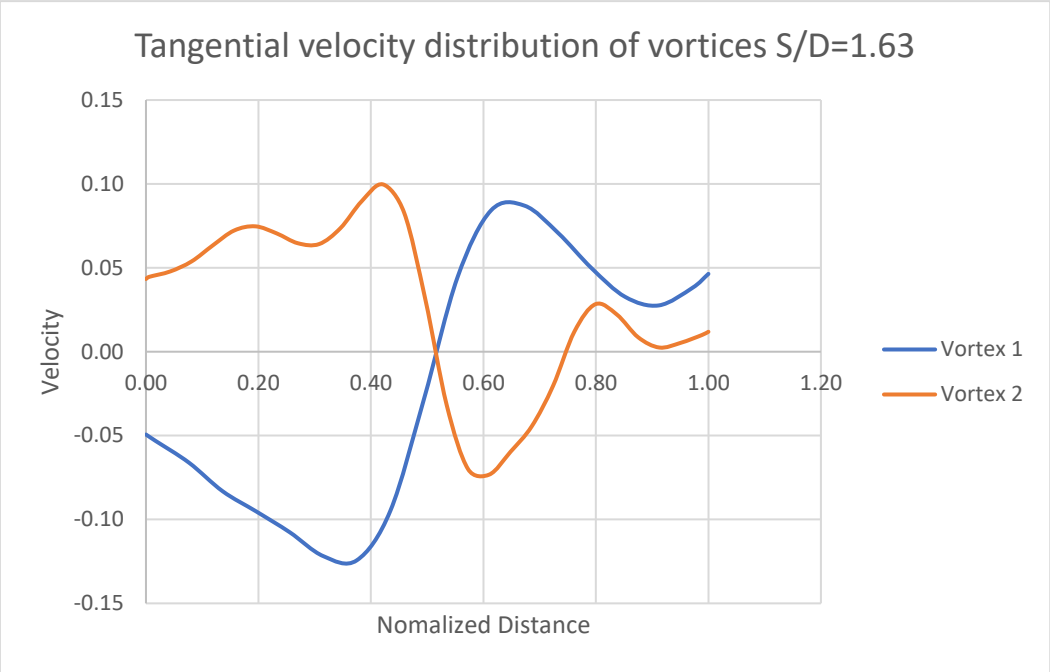

Figure 4- 19: Tangential velocity distributions along the radial distance in the vortices formed during submergence level of S/D=1.63

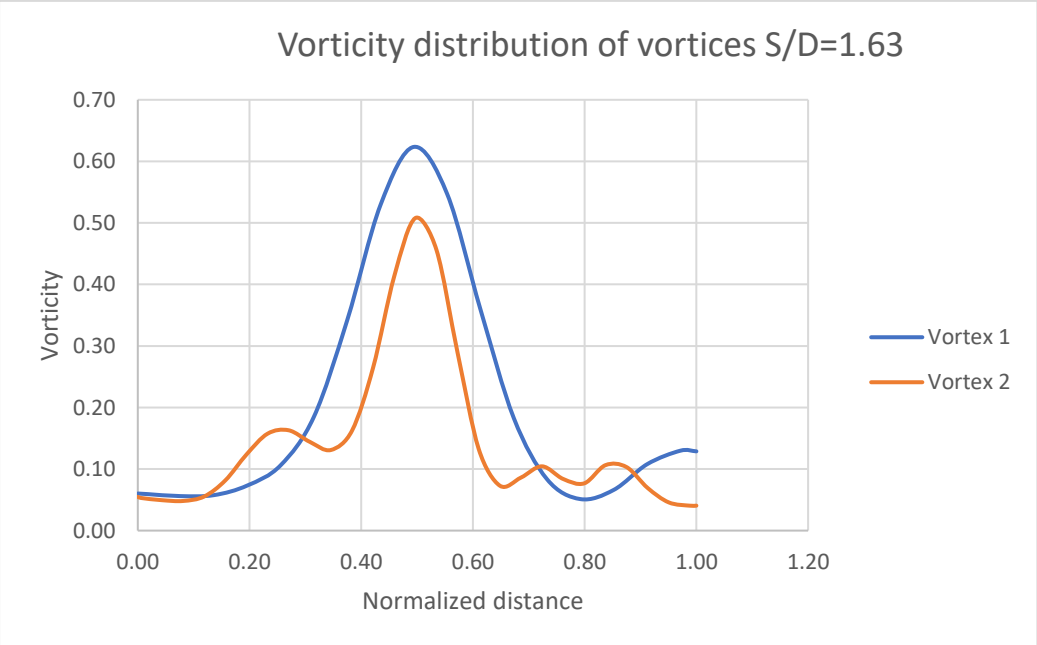

Figure 4- 20: Vorticity distribution of the same submergence level along the radial distance

Figure 4.21. illustrates the streamline arrangement of vortices in S/D=1.63

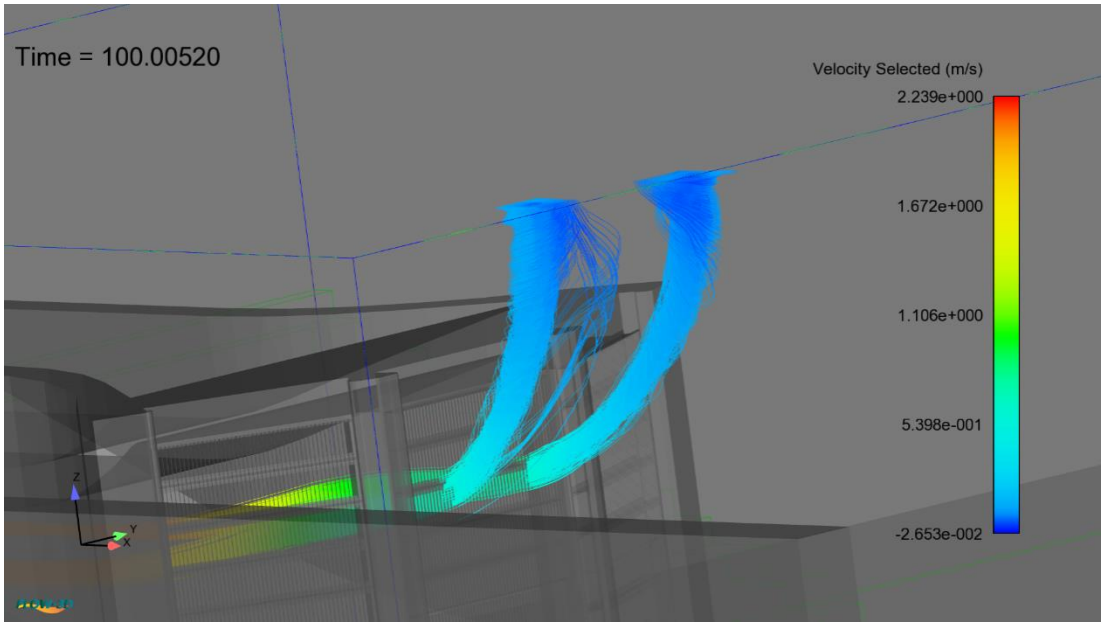

Figure 4- 21: Streamline arrangement of vortices in S/D=1.63

4.2.2. Flow pattern through the intake structure

The same numerical model is used to study the flow pattern through the intake structure, in order to identify the design drawbacks and possible modifications related to minimizing the vorticity problem. When compared to the intake geometries, discussed in [37], the Samanala hydropower intake has a different geometry. The intake bell-mouth does not continue to the front face of the intake. Instead, a flat deck is built, as the top of the intake guiding to the front face. The side walls of the intake have a curved profile. The bottom of the intake also has a flat deck without a curved profile. The velocity distribution of the cut plane through the y=0 (the center line of the intake) is given in Figure 4-22.

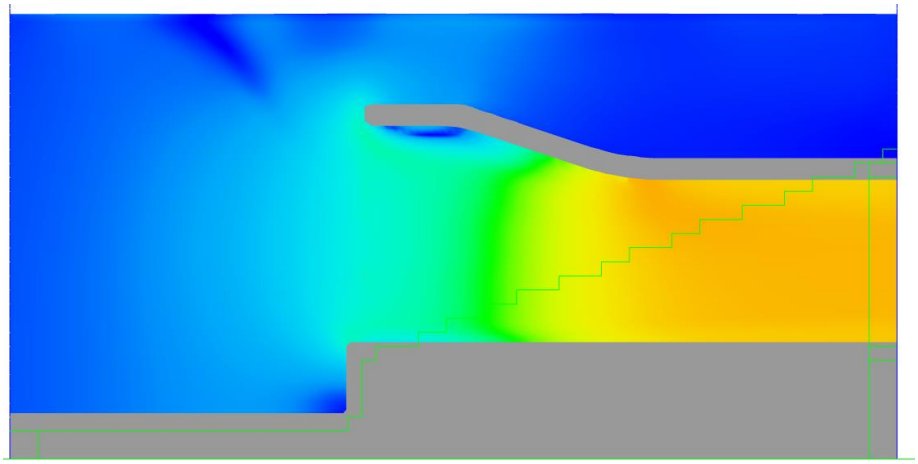

Figure 4- 22: Velocity Distribution in a vertical plane through the centerline of the intake

It can be clearly identified that; the horizontal top deck of the intake structure does not follow the flow pattern from the intake, before it reaches the bell-mouth. This creates a high vorticity area, underneath the top deck of the intake, and therefore elevates the intake head loss. Figure 4-23 illustrates the velocity distribution inside the intake at y=0 plane and along a vertical distance from intake bottom to the top. The velocity drastically drops near the soffit of the horizontal top deck.

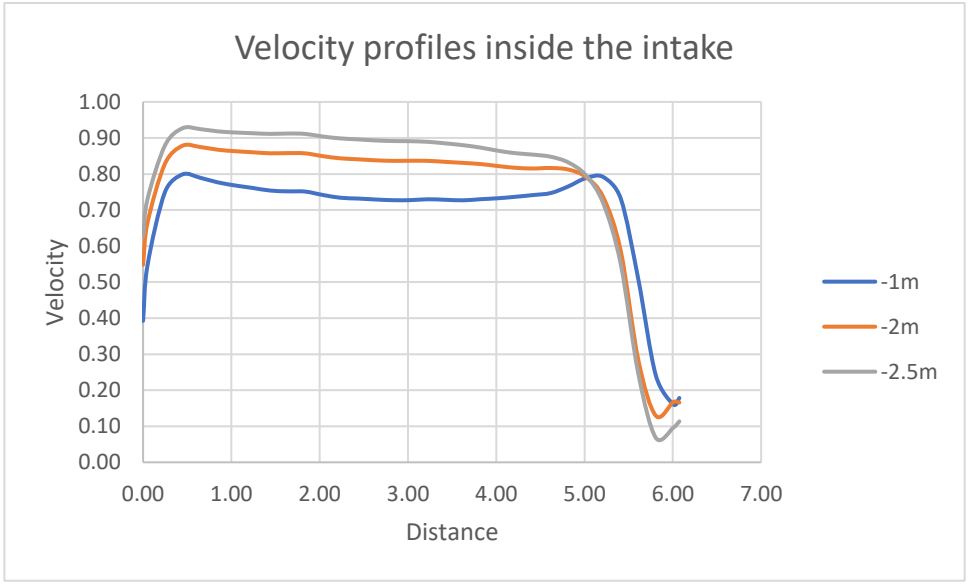

Figure 4- 23: Velocity distribution inside the Intake from bottom to the top, at different distances along -X direction

The front edge of the deck disturbed and separated the flow into these two zones. This creates a dead zone underneath the top deck, where water velocity is very low. Figure 4-24 illustrates the vorticity distribution in the same cut plane. The vorticity underneath the top deck is very high due to the flow separation.

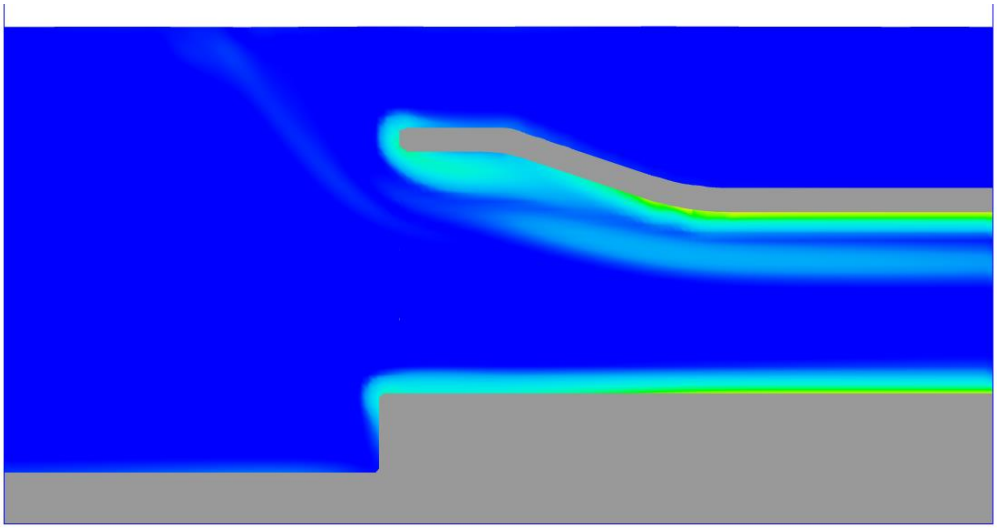

Figure 4- 24: Vorticity distribution in a vertical plane through the centerline of the intake

Furthermore, due to the disturbance of the flow towards the intake by horizontal top deck, the dead zone above the intake is larger. Figure 4-22 illustrates the separation of shear layer, in-between funnel shape flow, towards the intake and the dead zone where water velocities are lesser. This dead zone can be easily transformed to create a vortex due to its low velocities.

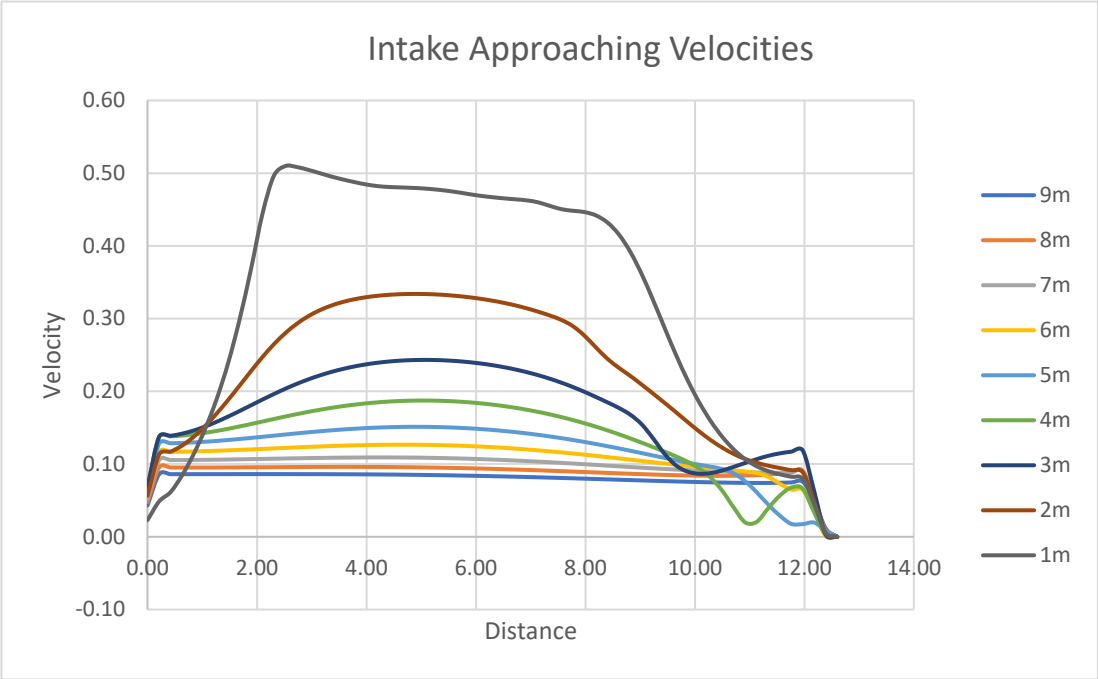

Figure 4- 25: Flow velocity distribution towards the intake work

Figure 4-25 illustrates the flow velocity distributions towards the intake works. Velocity distributions, along different lines perpendicular to the y=0 cut planes and starting from bottom of the pond to the free surface, are generated and plotted in the same graph. It can be clearly identified that the velocity near the free surface to the depth of 1m, is having approximately equal velocities, when approaching the flow of the intake. When flow approaches the intake, the funnel shape increases the flow velocity creating a lower velocity field (Dead zone) above the intake area. This dead zone creates vortices when the volume of water cannot resist the rotation of the streamlines [28].

CHAPTER 5. CONCLUSIONS AND FUTURE WORK

Formation of vortices at hydropower intakes is an undesirable phenomenon which drops down the total efficiency of the system. Samanala hydropower intake has undergone several modifications owing to the recent rehabilitation projects. Several undesirable physical phenomena, such as free surface vortex formation, frequent blockage and sedimentation at the intake work, have been observed. Formation of free surface vortices at the Samanala hydropower intake was studied with the present work using computational fluid dynamic software Flow-3D.

Numerical simulation can be successfully used to predict the vortex formation in hydropower intakes. Depending on the model, some of the features of the vortex may not be captured, for example, in the present study the free surface depression was not captured by the numerical model. However, the present model which was modeled using the Flow-3D CFD package, was able to correctly estimate the Parameters and characteristics of the free surface vortices at horizontal type hydropower intake of Samanala Power Station.

Validation of the numerical model is an important factor in computational fluid dynamics. The present model was validated using a physical model, built to match the functional requirements of the horizontal type protruded intake. The scale of the physical model is a vital factor when using Flow 3D software. The time step size and the meshing flexibilities are reduced when dealing with smaller scale models. The model built for the present study was also not adequate in scale, in order to use higher time steps and larger element sizes in meshing, which ended up with higher simulation time and computational power.

The critical submergence levels were tested using the model under constant flow rate of 36.4m^3/s, which is the highest possible flow rate through the intake. Most of the simulations formed two bidirectional rotating vortices, which can be an inherent characteristic of the intake work. The vorticity measurements of the vortices are increased with the decreasing submergence level of the intake. The maximum

vorticity of the vortices formed was laid between 1.05 to 0.2 1/s. The vortex appearing time is longer for higher submergence levels, while formation of vortices in the lower submergence level is not steady but repetitive. It was identified that the vortex occurrence point is moving outward to the intake work with the increase of the submergence level. This is because of the increasing dead zone area due to funnel shape approaching flow.

The characteristics of the approaching flow to the intake are studied. The flow characteristics are influenced by the underrated intake design. The flat top deck of the intake disturbed the flow, and increased the dead zone above the intake. Intake entrance is not at its Optimum hydraulic shape. Optimization of the top hydraulic profile of the intake will reduce the possibility of forming free surface vortices and elevate the operating submergence range of the intake.

It is not possible to estimate the amount of air entrance with this numerical model. Hence, a model has to be developed to accommodate the surface depression and the air entrance. High dense mesh and the longer simulations must be utilized for this purpose. The effect of the trash rack profiles and the clear spacing of the trash racks to the formation of vortices are areas to be studied further. Very fine mesh is required to model the trash rack area of the intake, which requires higher computational power and time.

The model can be used to investigate the free surface vortices in surge shafts and intake gate shafts of hydropower stations. The Intake gate shaft has a lower static head, when compared to the static head before the intake, and due to the intake head loss. Hence there is a possibility to form free surface vortices inside the gate shaft due to the lower submergence level.

Present study evaluates the vortex formation of the intake structure without considering the surrounding factors, such as level of sedimentation and the approaching slope of the pond, and in order to simplify the analysis. This study can be expanded to analyze the vortex formation of Samanala Intake with exact contour

map (Bathymetric Surveyed map) of the pond with present condition, which will estimate the vortex formation with higher accuracy.

REFERENCES

[1] Laxapana Power Station, Ceylon Electricity Board, *Reservoir Level Reading Book*, Laxapana: Laxapana Power Station, 2018.

[2] D. Bratko and A. Doko, "Water Intake Structures for Hydropower," in *2nd International Balkans Conference on Challenges of Civil Engineering*, Albania, 2013.

[3] Samanala Power Station, Ceylon Electricity Board, *Polpitiya Power Unit Transient Calculation*, VOITH, 2015.

[4] Laxapana Power Station, Ceylon Electricity Board, *Drawing-Erection for Trash Racks*, Vancouver: Canada Iron, 1966.

[5] J. Knauss, Swirling Flow Problems at Intakes, Rotterdam: A. A. Balkema, 1987.

[6] G. Hecker, "Model-Prototype comparion of free surface vortices," *Journal of The Hydraulics Division*, vol. 107, no. ASCE, USA, pp. 1243-1259, 1981.

[7] W. W. Durgin and G. E. Hecker, "The Modeling of Vortices in Intake Structures," in *Proc IAHR-ASME-ASCE Joint Symposium on Design and Operation of Fluid Machinery*, CSU Fort Collins, 1978.

[8] H. O. Anwar and J.A. Weller , "Similarity of free-vortex at horizontal intakes," *Journal of Hydraulic Research*, vol. 16 (2), no. ASME, pp. 95-105, 1978.

[9] A. Hribernik, M. Fike and T. M. Hribern, "Economical Optimization of a Trashrack Design for a Hydropower Plant," *Journal of Trends in the Development of Machinery and Associated Technology*, vol. 17, no. ISSN 2303-4009 (online), pp. 161-164, 2013.

[10] Public Utilities Commission of Sri Lanka, "Generation Performance in Sri Lanka 2016," Public Utilities Commission of Sri Lanka, Colombo, 2016.

[11] Japan International Cooperation Agency (JICA), Ceylon Electricity Board (CEB), "The follow-up study on the rehabilitation of hydropower stations in the Kelani river basin for hydropower optimization in Sri Lanka Vol I," Electric Power Development Co., LTD, Tokyo, 2006.

[12] Wu J. Z., Ma H. Y. and Zhou M. D. , Vorticity and Vortex Dynamics, USA: Springer, 2006.

[13] D.J. Acheson, Elementary Fluid Dynamics, USA: Oxford University Press, 1990.

[14] S.I. Green, Fluid Vortices, Dordrecht: Kluwer Academic Publishers, 1995.

[15] A. Ogawa, Vortex Flow, Florida: CRC Press, 1993.

[16] J. F. Douglas, J. M. Gasiorek and J. A. Swaffield, Fluid Mechanics, India: Pearson Education (Singapore) Pte Ltd, 2002.

[17] R. Mayer, Introduction to mathematical fluid dynamics, New York: Dover publication inc., 1982.

[18] O. Kiviniemi and G. Makusa, "A Scale model investigation of free surface vortex with particle tracking velocimetry," Lulea University of Technology, 2009.

[19] R. Ettema, R. Arndt, B. Roberts and T. Wahl, "Hydraulic Modeling: Concepts and Practice," ASCE, USA, 2000.

[20] P. Novak , C. Nalluri and A. I. B. Moffat, "Hydraulic Structures," Taylor & Francis, 2007.

[21] Anderson and L. David, Computational Fluid Dynamics, McGraw-Hill, Inc, 1995.

[22] Caminha and Guilherme, "The CFL condition and how to choose your timestep size," Simscale, 13 March 2018. [Online]. Available: www.simscale.com. [Accessed April 2018].

[23] V. P. Rajendran, G. S. Constantinescu and V. C. Patel, "Experiments on flow in a model water-pump intake sump to validate a numerical model," in *FEDSM'98 ASME Fluid Engineering Division Summer Meeting*, Washington, 1998.

[24] F. Suerich-Gulick, S. Gaskin, M. Villeneuve, G. Holder and E. Parkinson, "Experimental and numerical analysis of free surface vortices at a hydropower intake," in *Conference on Hydroscience and Engineering*, Philadelphia, USA, 2006.

[25] A. Skerlavaj, L. Skerget, J. Ravnik and A. Lipej, "Predicting Free-Surface Vortices with Single Phase Simulations," *Engineering Applications of Computational Fluid Mechanics*, vol. 8, no. 2, pp. 193-210, 2014.

[26] C. Lucino , S. Liscia and G. Duro, "Vortex detection in pump sumps by means of CFD," in *XXIV Latin American Congress Hydraulics Punta Del Este*, Uruguay, 2010.

[27] A. C. Bayeul-Laine, S. Simonet, A. Issa and G. Bois, "The importance of the knowladge of flow stream in water sump pump," in *Congres Francais de Mecanique*, 2013.

[28] H. Sarkardeh, A. R. Zarrati, E. Jabbari and M. Marosi, "Numerical Simulation and Analysis of Flow in a Reservoir in the presence of Vortex," *Engineering Applications of Computational Fluid Mechanics*, vol. 8, no. 4, pp. 598-608, 2014.

[29] American Society of Civil Engineers, Committee on Hydropower Intakes, "Guidelines for design of intakes for hydroelectric plants," American Society of Civil Engineers, USA, 1995.

[30] J. S. Gulliver and A. J. Rindels, "Weak vortices at vertical intakes," *Journal of Hydraulic Engineering*, vol. 113, no. 9, 1987.

[31] A. K. Jain, K. G. Ranga Raju and R. J. Garde, "Vortex formation of Vertical pipe intakes," *ASCE Hydraulic Division*, vol. 104, no. HY10, 1978.

[32] Moreno, J. Carlos and Gavilan, "Determining critical submergence in tanks by means of Reynolds & Weber Numbers," *World Journal of Engineering and Technology,* vol. 2, no. 3, pp. 222-233, 2014.

[33] J. Yang, T. Liu, A. Bottacin-Busolin and C. Lin, "Effects of intake-entrance profiles on free-surface vortices," *Journal of Hydraulic Research,* vol. 52, no. 4, pp. 523-531, 2014.

[34] C.W. Hirt and B.D. Nichols, "Volume of Fluid Method for the Dynamics of Free Boundaries," *Journal of Computational Physics,* vol. 39, pp. 201-225, 1981.

[35] Flow Science Inc., "Flow-3D Tutorial/Quick Start," Flow Science Inc., [Online]. Available: file:///C:/flow3d/v11.2/help/tutorial.html.

[36] National Hydrographic Office, National Aquatic Resources Agency (NARA), *Hydrographic Survey of Laxapana Pond for Ceylon Electricity Board,* Colombo: National Aquatic Resources Agency (NARA), 1987.

[37] H.K. Blair and T.J. Rhone, "Outlet Works," in *Design of Small Dams*, New Delhi, SBS Publishers & Distributors (Pvt) LTD, 2006, pp. 435-489.